# First 17−18−19-Electron Triads of Stable Isostructural Organometallic Complexes. The 17-Electron Complexes $[Fe(C_5R_5)(arene)]^{2+}$ (R = H or Me), a Novel Family of Strong Oxidants: Isolation, Characterization, Electronic Structure, and Redox Properties

**Jaime Ruiz,[†] François Ogliaro,[‡] Jean-Yves Saillard,*[,‡] Jean-François Halet,[‡] François Varret,[§] and Didier Astruc*[,†]**

*Contribution from the Groupe de Chimie Supramoléculaire des Métaux de Transition, LCOO, UMR CNRS No. 5802, Université Bordeaux I, 33405 Talence Cedex, France, Laboratoire de Chimie du Solide et Inorganique Moléculaire, UMR CNRS No. 6511, Université de Rennes 1, 35042 Rennes Cedex, France, and Laboratoire de Magnétisme et d'Optique, URA CNRS No. 1531, Université de Versailles, 78035 Versailles Cedex, France*

*Received July 6, 1998*

**Abstract:** The 18-electron complexes $[M^{II}(C_5R_5)(arene)]^+$ (M = Fe: R = H or Me, arene = $C_6H_{6-n}Me_n$ ($n$ = 0−6), $C_6H_5NMe_2$, or $C_6Me_5NH_2$; M = Ru: R = Me, arene = $C_6Me_6$) are oxidized to $M^{III}$ complexes between 0.92 and 1.70 V vs $[FeCp_2]$ according to a single-electron process that is reversible in $SO_2$ if at least one of the rings is permethylated. The dinuclear complex $[Fe^{II}_2(fulvalenyl)(C_6Me_6)][PF_6]_2$ is oxidized in two one-electron reversible waves in $SO_2$ separated by 0.38 V to the mixed-valence species trication and to the 34-electron dioxidized tetracation. Stoichiometric oxidation of the yellow complexes $[Fe^{II}Cp^*(arene)][EX_6]$ ($EX_6$ = $PF_6$ or $SbCl_6$) is achieved by using $SbCl_5$ in $CH_2Cl_2$ at 20 °C or $SbF_5$ in $SO_2$ at −10 °C or by $Br_2$ + $[Ag][SbF_6]$ and gives the purple 17-electron complexes $[Fe^{III}Cp^*(arene)][SbX_6]_2$ (X = F or Cl) if arene = hexa-, penta-, and 1,2,4,5-tetramethylbenzene. No oxidation is observed for complexes of less methylated arene ligands, which shows that the oxidation power of $SbX_5$ is limited to 1.0 V *vs* $[FeCp_2]$ for monocations. The complex $[Fe^{III}Cp^*(C_6Me_6)][SbCl_6]_2$, **1**$[SbCl_6]_2$, is also obtained by $SbCl_5$ oxidation of the 19-electron complex $[Fe^{I}Cp^*(C_6Me_6)]$, **1**, at −80 °C. The 17-electron complexes are characterized by elemental analyses, ESR, Mössbauer, and UV/vis spectra, magnetic susceptibility, cyclic voltammetry, and quantitative single-electron reduction by ferrocene. The complex **1**$[SbCl_6]_2$ is used as a very strong single-electron oxidant to also oxidize $[Ru(bpy)_3][PF_6]_2$ to the 17-electron $Ru^{III}$ species and the neutral cluster $[FeCp(\mu_3\text{-}CO)]_4$ to its mono- and dications. The complex $[Fe^{II}Cp(C_6Me_6)][PF_6]$ is a redox catalyst for the anodic oxidation of furfural on Pt in $SO_2$ via the $Fe^{II}/Fe^{III}$ redox system. Density functional theory (DFT) calculations on various 17-electron compounds $[Fe(C_5R_5)(C_6R_6)]^{+/2+}$ (R = H, Me) and $[FeCp(C_6H_5NH_2)]^{2+}$, as well as on the isoelectronic complexes ferrocenium and $[Fe(C_6H_6)_2]^{3+}$ and their 18-electron parents, allowed a detailed comparison of the electronic structure, bonding, UV−visible spectra, and ionization potentials of these species. Although the nature of the HOMO is not always the same within the series of their 18-electron parents, all the computed 17-electron complexes have the same $^2E_2$ ground state corresponding to the metallic $(a_1)^2(e_2)^3$ electron configuration. Full geometry optimizations lead to the prediction of their molecular structures for the lowest $^2E_2$ and $^1A_1$ states.

## Introduction

Since its discovery 45 years ago, the 17-electron complex ferrocenium[1] has been the subject of considerable popularity as a single-electron oxidant despite the modest value of the ferrocene/ferrocenium oxidation potential (0.44 V vs SCE in $CH_2Cl_2$).[2,3] Although various ferrocene derivatives with electron-withdrawing substituents are known to have more positive redox potentials, only acetylferrocenium has been used as an oxidant ($E°$ = 0.27 V vs $[Cp_2Fe]^{0/+}$ in $CH_2Cl_2$ or MeCN).[2−4] Increasing the charge by one unit without changing the number of valence electrons is a way to shift the redox potential toward more positive values by more than 1 V. In this respect, the 17-electron $[FeCp(arene)]^{2+}$(Cp = $\eta^5$-$C_5H_5$), isolobal with ferrocenium, have neither been detected by electrochemistry nor isolated, which attracted our attention. Since we know that 19-electron complexes of this series were stabilized by steric protection with a shell of methyl substituents on the ligands

[†] Université Bordeaux I.
[‡] Theoretical studies: Université de Rennes 1.
[§] Mössbauer studies: Université de Versailles.

(1) Wilkinson, G.; Rosenblum, M.; Whiting, M. C.; Woodward, R. B. *J. Am. Chem. Soc.* **1952**, *74*, 2125.
(2) (a) Connelly, N. G.; Geiger, W. E. *Chem. Rev.* **1996**, *96*, 877. (b) Connelly, N. G.; Geiger, W. E. *Adv. Organomet. Chem.* **1984**, *23*, 1. (c) Geiger, W. E. *J. Organomet. Chem. Libr.* **1990**, *23*, 142.
(3) (a) Astruc, D. *Electron-Transfer and Radical Processes in Transition-Metal Chemistry*, VCH: New York, 1995. (b) Reference 3a, Chapter 2.
(4) Kuwana, T.; Bublitz, D. E.; Hoh, G. *J. Am. Chem. Soc.* **1960**, *82*, 5811.

10.1021/ja982342z CCC: $15.00 
Published on Web 10/28/1998

around the metal center,[3] we anticipated that an analogous strategy concerning the oxidation side might similarly lead to the stabilization of highly oxidizing 17-electron complexes. In a useful range of redox potentials around 1 V vs $[Cp_2Fe]^{0/+}$, several oxidants such as $[Fe^{III}(bpy)_3]^{3+}$,[5] $Ce^{IV}$amonium nitrate (CAN),[6] $Mn^{IV}$pyrazolyl complexes,[7] and $NAr_3^{\bullet+}$ [8] are already known. Seminal studies by Bard's group have even shown that it is possible to synthesize electrochemically high-oxidation-state species such as $[M(bpy)_3]^{4+}$ (M = Ni or Ru) whose redox potentials are more positive than 1.5 V vs $[Cp_2Fe]^{0/+}$.[9] Interestingly, the most oxidizing species ever used in single-oxidation chemistry is Bartlett's salt $[O_2][PtF_6]$ (or other dioxygenyl salts)[10−14] discovered in 1962.[10] Electron−hole formation is increasingly being exploited in organic[8,13,15] and inorganic chemistry.[16] For instance, it has recently been shown by Reed *et al.* that $C_{76}$[16a] and even $C_{60}$[16b,c] could be cleanly oxidized to their monocations.

The $[M^{II}Cp(arene)]^+$ salts (M = Fe or Ru) are so robust toward oxidation of the $M^{II}$ center (by common oxidizing agents) that NMR studies of the $Fe^{II}$ complexes have been carried out in concentrated $D_2SO_4$,[17] and it was commonly believed that these complexes could not be oxidized.[18] In a preliminary communication, Solodovnikov *et al.* reported in 1980 the low-temperature generation using $SbCl_5$ and ESR spectra of unstable oxidized species from $[FeCp(arene)]^+$ complexes bearing either an anisole or polyaromatic ligand.[19a] These authors proposed, for these species, a 17-electron structure.[19b] No electrochemical or other analytical or spectroscopic data were given in this communication, however. To our knowledge, there is no other report on the oxidation of the complexes of the $[FeCp(arene)]^+$ family.

We now report for the first time (i) the electrochemical single-electron oxidation of the 18-electron complexes $[M^{II}(C_5R_5)(arene)]^+$ (M = Fe or Ru; R = H or Me)[20] at very high potentials with various arenes, (ii) the oxidation of the polymethylated complexes in this series (R = Me, arene = durene, pentamethylbenzene, and hexamethylbenzene) with $SbCl_5$ in $CH_2Cl_2$ at 20 °C or $SbF_5$ in liquid $SO_2$ at −40 °C including a quite accurate indication of the oxidizing power of $SbCl_5$ and $SbF_5$ toward monocations, (iii) the analytical and spectroscopic characterization (Mössbauer, ESR, UV/vis, magnetic moment, cyclic votammetry) of these 17-electron $d^5$ complexes $[FeCp^*(arene)]^{2+}$ ($Cp^* = \eta^5$-$C_5Me_5$), (iv) the prediction of their molecular structure and the investigation of their electronic structure using density functional theory (DFT) together with a comparison with the electronic structures of the isoelectronic symmetrical 17-electron iron-sandwich complexes ferrocenium and $[Fe(C_6H_6)_2]^{3+}$, and finally (v) a few examples illustrating the use of the fully methylated 17-electron complex $[Fe(C_5Me_5)(C_6Me_6)][SbCl_6]_2$ in oxidation chemistry including the first synthesis of the dication of the well-known cluster $[FeCp(\mu_3\text{-}CO)]_4$.

## Results and Discussion

**Cyclic Voltammetry on the Oxidation Side of the 18-Electron $[M(C_5R_5)(arene)]^+$ Complexes (R = H or Me; M = Fe or Ru).** The analytical electrochemistry of the $[FeCp(arene)]^+$ complexes on the reduction side has been known for a long time to give two single-electron reductions and has been thoroughly studied.[2,3b] We have now recorded the unknown anodic oxidation of various $[M(C_5R_5)(arene)]^+$ complexes (M being mostly Fe) by cyclic voltammetry at very high potentials in liquid $SO_2$, MeCN, and $CH_2Cl_2$, and the results are summarized in Table 1. In $SO_2$ at −40 °C, the oxidation wave is chemically and electrochemically reversible if at least one of the rings is permethylated (Figures 1a and 1b).

We have also recorded for comparison the redox potentials of the complexes $[Cr(arene)(CO)_3]$ (arene = benzene, mesitylene, and hexamethylbenzene) whose single-electron oxidation is also reversible.[21] Although the oxidation potentials of our cationic iron complexes are about 1 V more positive than those of the chromium series, this difference does not really reflect the respective electron-withdrawing influences of the two 12-electron fragments $FeCp^+$ (or $FeCp^{*+}$) and $Cr(CO)_3$ on the arene, since the electron is not removed from an arene orbital but from a nonbonding metal orbital in both cases (*vide infra*). Thus, oxidation of the iron, ruthenium, and chromium complexes is easier than oxidation of the free aromatic molecules. For instance, $C_6Me_6$ is oxidized at 1.6 V vs $[FeCp_2]$,[22a] *i.e.* at a potential 0.6 V more positive than its $Cp^*Fe^+$ complex. To obtain a reliable and accurate measurement of the influence of the methyl groups on the redox potential, we have also recorded the voltammogram of a mixture of ferrocene, $[FeCp^*(C_6H_6)][PF_6]$, $[FeCp^*(mesitylene)][PF_6]$, and $[FeCp^*(C_6Me_6)][PF_6]$, which shows that the redox potential becomes less positive by $\Delta E° = 60$ mV for each added methyl group. This compares to 120 mV for the free arene series and to 40 mV in the $[Cr(arene)(CO)_3]$ series (Table 1).

(5) (a) Wong, C. L.; Kochi, J. K. *J. Am. Chem. Soc*. **1979**, *101*, 5593. (b) $[Fe(bpy)_3]^{3+}$ has been used as an oxidant to determine the number of hydride ligands in hydride complexes: Lemmen, T. H.; Lundquist, E. G.; Rhodes, L. F.; Sutherland, B. R.; Westerberg, D. E.; Caulton, K. G. *Inorg. Chem*. **1986**, *25*, 3915.

(6) Bard, A. J.; Faulkner, L. R. *Electrochemical Methods*; Wiley: New York, 1980; p 699.

(7) Chan, M. K.; Armstrong, W. H. *Inorg. Chem*. **1989**, *28*, 3777.

(8) (a) Steckhan, E. *Top. Curr. Chem*. **1987**, *142*, 1. (b) Steckhan, E. *Angew. Chem., Int. Ed. Engl*. **1986**, *25*, 683.

(9) (a) Chlistunoff, J. B.; Bard, A. J. *Inorg. Chem*. **1992**, *31*, 4582. (b) Sharp, P. R.; Bard, A. *Inorg. Chem*. **1983**, *22*, 2689. (c) Bard, A. J.; Garcia, E.; Kukharenko, S.; Strelets, V. V. *Inorg. Chem*. **1993**, *32*, 3528.

(10) Bartlett, N.; Lohmann, D. H. *J. Chem. Soc*. **1962**, 5253.

(11) Dioxygen has a higher ionization potential (12.1 eV) than xenon (11.6 eV). It is when he succeeded in making $[O_2][PtF_6]$ that Bartlett had the wonderful idea to make what became the first rare-gas compound $[Xe][PtF_6]$.[10.]

(12) Dioxygenyl salts were used to oxidize other substrates which are very difficult to oxidize[12a,b,13] (a) Richardson, T. J.; Bartlett, N. *J. Chem. Soc., Chem. Commun*. **1974**, 427. (b) Zücher, K.; Richardson, T. J.; Glemser, O.; Bartlett, N. *Angew. Chem., Int. Ed. Engl*. **1980**, *19*, 944.

(13) Dinnocenzo, J. P.; Banach, T. E. *J. Am. Chem. Soc*. **1986**, *108*, 6063; **1988**, 110, *971*; **1989**, *111*, 8646.

(14) (a) The $O_2/O_2^{\bullet+}$ oxidation potential has been estimated to be 5.3 V vs SCE. This calculation arises from the value of the ionization potential (12.08 eV),[14b] application of Miller's equation,[13,14c] and adding 0.34 V to convert the value so obtained to the SCE potential. (b)Turner, D. W.; May, D. P. *J. Chem. Phys*. **1966**, *45*, 471. (c) Miller, L. L.; Nordblom, G. D.; Mayeda, E.A. *J. Org. Chem*. **1972**, *37*, 916.

(15) (a) Bauld, N. L. *Advances in Electron-Transfer Chemistry*; Mariano, P. S., Ed.; JAI Press: Greenwich, CT, 1992; Vol. 2. (b) Mattay, J.; Vonderhof, M. *Top. Curr. Chem*. **1991**, *159*, 219.

(16) (a) Bolskar, R. D.; Mathur, S.; Reed, C. A. *J. Am. Chem. Soc*. **1996**, *118*, 13093. (b) Reed, C. A. *Acc. Chem. Res*. **1998**, *31*, 133. (c) Dagani, R. *Chem. Eng. News* **1998**, *May 4*, pp 49−54.

(17) Lee, C. C.; Demchuk, K. J.; Sutherland, R. G. *J. Organomet. Chem*. **1979**, *57*, 933.

(18) Nesmeyanov, A. N. *Adv. Organomet. Chem*. **1972**, *10*, 1.

(19) (a) Solodovnikov, S. P.; Nesmeyanov, A. N.; Vol'kenau, N. A.; Kotova, L. S. *J. Organomet. Chem*. **1980**, *201*, C45. (b) Alternatively, oxidation of the aromatic ligand may have occurred (oxidation of complexes of simple arenes could not be achieved by these authors).

(20) Reviews on 18-electron monocationic $[FeCp(arene)]^+$ complexes: (a) Astruc, D. Tetrahedron Report No. 157. In *Tetrahedron* **1983**, *39*, 4027. (b) Astruc, D. *Top. Curr. Chem*. **1991**, *160*, 47.

(21) (a) Zoski, C. G.; Sweigart, D. A.; Stone, N. J.; Rieger, P. H.; Mocellin, E.; Mann, T. F.; Mann, D. R.; Gosser, D. K.; Doeff, M. M.; Bond, A. M. *J. Am. Chem. Soc*. **1988**, *110*, 2109. (b) Yeung, L. K.; Kim, J. E.; Rieger, P. H.; Sweigart, D. A. *Organometallics* **1996**, *15*, 3891.

(22) (a) Lehmann, R. E.; Kochi, J. K. *J. Am. Chem. Soc*. **1991**, *113*, 501. (b) Vlcek, A. A. *Z. Anorg. Chem. Allg. Chem*. **1960**, *304*, 109.

**Table 1.** Oxidation Potentials $E_{1/2}$ (V) of the Complexes $[M(C_5R_5)(arene)]^{+/2+}$ (M = Fe or Ru, R = H or Me) and $[Cr(arene)(CO)_3]$ *vs* $[FeCp_2]^{0/+}$ (by cyclic voltammetry)[a]

| | $SO_2$ (−40 °C) | | MeCN | | |
|---|---|---|---|---|---|
| | | | | $i_c/i_a$ | |
| | $E_{1/2}$ (V) | $i_c/i_a$ | $E_{1/2}$ (V) | −20 °C | +20 °C |
| $[FeCp(C_6H_6)]^+$ | $E_{pa} = 1.700$[b] | 0 | | | |
| $[FeCp(mesitylene)]^+$ | $E_{pa} = 1.490$[b] | 0 | | | 0 |
| $[FeCp(C_6Me_6)]^+$ | 1.280 | 1 | 1.250 | 0 | 0 |
| $[FeCp(p.Me\text{-}C_6H_4\text{-}NH_2)]^+$ | 0.995 | 1 | 1.113 | 0 | 0 |
| $[FeCp(C_6Me_5NH_2)]^+$ | 0.950 | 1 | 0.865 | 0.4 | 0 |
| $[FeCp^*(C_6H_6)]^+$ | 1.290 | 1 | 1.135 | 1 | 0 |
| $[FeCp^*(p\text{-xylene})]^+$ | 1.165 | 1 | 1.080 | 1 | 0 |
| $[FeCp^*(mesitylene)]^+$ | 1.105 | 1 | 1.010 | 1 | 0 |
| $[FeCp^*(durene)]^+$ (**4**$^+$) | 1.045 | 1 | 0.985 | 1 | 0 |
| $[FeCp^*(C_6HMe_5)]^+$ (**2**$^+$) | 0.985 | 1 | 0.925 | 1 | |
| $[FeCp^*(C_6Me_6)]^+$ (**1**$^+$) | 0.920 | 1 | | | |
| $[FeCp^*C_6H_5NH(CH_2)_2CH_3]^+$ | 0.800 | 1 | 0.780 | 0 | 0 |
| $[RuCp^*(C_6Me_6)]^+$ | 1.530 | 0.8 | | | |
| $[Fe_2(fulvalenyl)(C_6Me_6)_2]^{2+}$ (**3**$^{2+}$) | 1.330 | 1 | | | |
| (see Figure 3 for **3**$^{2+}$) | 1.710 ($\Delta E_p$ = 60 mV) | 1 | | | |
| $[Cr(C_6H_6)(CO)_3]$ | | | 0.420 | 0 | 0 |
| $[Cr(mesitylene)(CO)_3]$ | | | 0.305 | 0.4 | 0 |
| $[Cr(C_6Me_6)(CO)_3]$ | | | 0.180 | 1 | 1 |

[a] Internal reference: $[FeCp_2]$; $[n\text{-}Bu_4N][PF_6]$ 0.1 M on Pt anode. $E°([FeCp_2]^{0/+})$ SCE = 0.450 V in $SO_2$ ($\Delta E_p$ does not equal 40 mV) and 0.310 V in MeCN ($\Delta E_p$ does not equal 70 mV); counteranion: $PF_6^-$. For **1**$^+$ in $CH_2Cl_2$, $E_{1/2} = 1.030$ V *vs* $FeCp_2^{0/+}$; $E°(FeCp_2^{0/+})$ *vs* SCE = 0.440 V in $CH_2Cl_2$. [b] Scan rate: 0.2 V·s$^{-1}$ throughout the table. In $SO_2$, for the series $[FeCp^*(C_6Me_nH_{6-n})]^+$: $E_{1/2} = 1.290-0.060$ nV *vs* $[FeCp_2]^{0/+}$. In $CH_2Cl_2$, the oxidation of the complexes [Cr(arene)$(CO)_3$] (arene = benzene, mesitylene, hexamethylbenzene) is fully reversible.[21] The $E_{1/2}$ values for these complexes in $CH_2Cl_2$ are 0.420 (benzene), 0.310 (mesitylene), and 0.185 V (hexamethylbenzene) *vs* $[FeCp_2]^{0/+}$.

The ratio $\Delta E°$(complex)/$\Delta E°$(free arene) gives a qualitative indication of the ligand character in the HOMO,[22b] although it cannot be taken accurately.[23] Thus, the HOMO is a $z^2$ orbital in the [Cr(arene)$(CO)_3$] series without arene character and a minimum value of $\Delta E$ is found. This value is higher in the Fe series, consistent with the fact that there is some covalency for the ($xy$, $x^2-y^2$) metallic level involved in this case (13% arene character, vide infra).

The $E_{pa} - E_{pc}$ separation (40 mV) and the wave intensity (*vs* $[FeCp_2]$) indicated a chemically and electrochemically reversible single-electron oxidation to the $Fe^{III}$ dication. In MeCN, however, the chemical reversibility decreases from the fully methylated sandwich **1** to the less methylated ones (Table 1). For instance, the anodic oxidation of **1**$[PF_6]$ is chemically reversible at 20 °C in MeCN whereas that of $[FeCp^*(\eta^6\text{-}C_6Me_5H)][PF_6]$, **2**$[PF_6]$, is chemically fully irreversible at 20 °C. This shows the protection of the iron center by the methyl groups forming a cage in **1**$^{2+}$ and the great sensitivity toward nucleophilic attack by MeCN when a gate is open in the shell of methyl substituents as in **2**$^{2+}$.[24]

The complex **3**$[PF_6]_2$[25] is oxidized in $SO_2$ in two fully reversible one-electron waves at $E° = 1.330$ and 1.710 V *vs* $[FeCp_2]^{0/+}$ (Figure 2), which extends the redox cascade **3**$^x$ to seven oxidation states ($x = 2-$ to $4+$).

This large separation of 0.380 V might be in favor of an average-valence trication **3**$^{3+}$ [26] as it is in the case for **3**$^+$,[25] although spectroscopic studies are required to prove this. Anilines are oxidized at potentials about 1 V less positive than their $(C_5R_5)Fe^+$ complexes, which shows the strong electron-withdrawing character of this cationic 12-electron moiety. It is likely that the HOMO of a complexed aniline has a large contribution from the HOMO of the free amine, the oxidation of the complex involving removal of an electron from an orbital which has significant nitrogen lone-pair character. Interestingly, the DFT calculations (vide infra) also indicate a significant decoordination of the *ipso* carbon emphasizing the weight of the iminocyclohexadienyl mesomeric form (Chart 1).

The most easily oxidized complexes of the whole series are indeed $[FeCp(C_6Me_5NH_2)][PF_6]$ and $[FeCp^*(p\text{-}MeC_6H_4NMe_2)][PF_6]$. The effect of an amino group on the benzene ring on $E_{1/2}$ is slightly larger than that of the permethylation of either ring.

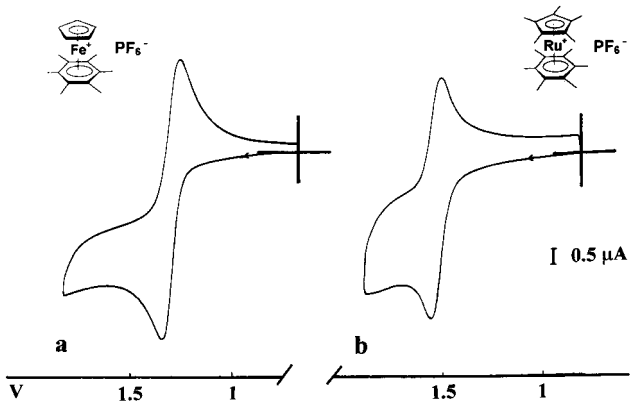


**Figure 1.** Cyclic voltammogram of (a) $[FeCp(C_6Me_6)][PF_6]$ in $SO_2$ at −40 °C and (b) $[RuCp^*(C_6Me_6)][PF_6]$ in $SO_2$ at −40 °C. Pt anode, $[n\text{-}Bu_4N][PF_6]$ 0.1 M, $[FeCp_2]$ as internal reference.

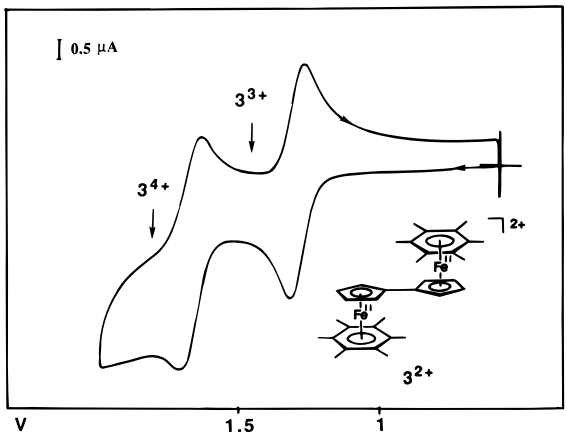


**Figure 2.** Cyclic voltammogram of **3**$[PF_6]_2$ in $SO_2$ at −40 °C. Pt anode, $[n\text{-}Bu_4N][PF_6]$ 0.1 M, $[FeCp_2]$ as internal reference; $E_{1/2} = 1.330$ and 1.710 V vs $[FeCp_2]$.

**Chart 1**

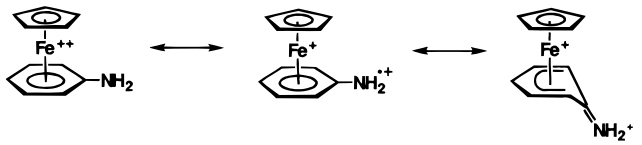


**Synthesis and Characterization of the [FeCp*-(arene)]$^{2+}$ Salts.** Oxidation of a soluble yellow salt **1**$[PF_6]$ or

(23) Lacoste, M.; Rabaâ, H.; Astruc, D.; Le Beuze, A.; Saillard, J.-Y.; Précigoux, G.; Courseille, C.; Ardoin, N.; Bowyer, W. *Organometallics* **1989**, *8*, 2233.

(24) Likewise, $[Fe^ICp(C_6Me_5H)]$ rapidly dimerizes at 20 °C whereas $[Fe^I\text{-}Cp(C_6Me_6)]$ is stable up to 100 °C: Hamon, J.-R.; Astruc, D.; Michaud, P. *J. Am. Chem. Soc.* **1981**, *103*, 758.

(25) Desbois, M.-H.; Astruc, D.; Guillin, J.; Varret, F.; Trautwein, A. X.; Villeneuve, G. *J. Am. Chem. Soc.* **1989**, *111*, 5800.

**Scheme 1**

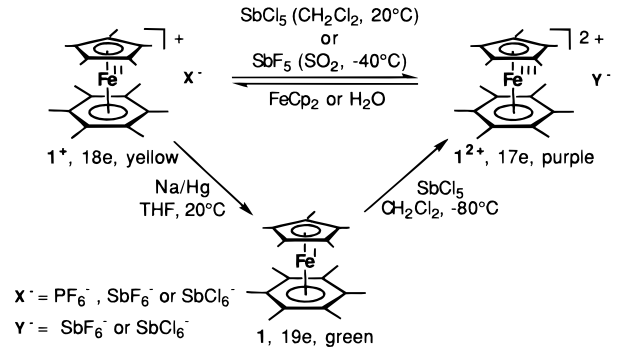


**1**[$SbCl_6$] in $CH_2Cl_2$ at 20 °C by excess $SbCl_5$ occurred instantaneously, yielding a purple precipitate of the $[SbCl_6]^-$ salt which was purified by washing with $CH_2Cl_2$ and recrystallized from $SO_2$ (70% yield). Metathesis of the anion eventually occurred (in the case of **1**[$PF_6$]) together with oxidation, so that the bis-$[SbCl_6]^-$ salt was obtained as reproducibly found by elemental analysis. Alternatively, single-electron reduction of $\mathbf{1}^+$ by Na/Hg in THF at 20 °C to its isostructural forest-green 19-electron form **1**[24,27] followed by extraction in pentane and addition of excess $SbCl_5$ in $CH_2Cl_2$ at −80 °C instantaneously gave a purple precipitate that was purified in the same way (70% yield from **1**, Scheme 1). This is the first example of an oxidation of a 19-electron complex to an isostructural 17-electron complex. It thus features a one-pot two-electron oxidation that mechanistically proceeds in two very distinct one-electron steps separated by 3 V!

This technique was originally applied *inter alia* to make sure that only $[SbCl_6]^-$ would be found as a counteranion, but it turned out that the same bis-$[SbCl_6]^-$ salt was obtained by using any of these two experimental procedures. The oxidation of **1**[$PF_6$] by $SbF_5$ in $SO_2$ at −40 °C also instantaneously occurred as the solution turned dark orange-brown without precipitate. After $SO_2$ was evaporated, the brown-purple residue was washed with $CH_2Cl_2$, leaving a purple solid, the bis-$[SbF_6]^-$ salt, which was recrystallized from $SO_2$. Finally, this purple complex could also be obtained by using Reed's technique, which consists of oxidizing the precursor with $Br_2$ in $CH_2Cl_2$ in the presence of a silver salt such as [Ag][$SbF_6$].[28] The measurement of the magnetic susceptibility by $^1$H NMR with Evans' method[29] gave $\mu = 2.40\ \mu$B. UV−vis absorptions in the spectrum recorded in MeCN at 20 °C were found for **1**[$SbCl_6$]$_2$ at 487 and 527 nm. These purple solids also were identified as salts of the $d^5$ 17-electron dication $\mathbf{1}^{2+}$ by elemental analysis, Mössbauer and ESR spectroscopies, and cyclic voltammetry in MeCN. The cyclic voltammogram of a purple MeCN solution of **1**[$SbCl_6$]$_2$ recorded at −30 °C is exactly the same as that of the yellow 18-electron monocationic salt.

**Mössbauer Spectroscopy.** The spectra were recorded under inert atmosphere at zero field and for various temperatures, and the changes in the spectra with temperature were found to be reversible. At room temperature, we observed a doublet with a small quadrupole splitting (Q.S.). On decreasing temperature, the spectrum was progressively distorted and, at low temperature, resulted in a broad asymmetrical line shape (Figure 3). This thermal variation is due to the slowing down of the electronic spin relaxation and agrees with the expected magnetic character (low spin, $s = {}^1/_2$) of the $3d^5$ electronic configuration. Such a thermal variation has been reported for some ferrocenium-type salts, even leading to a resolved magnetic sextet in the case of decamethylferrocenium salts.[30] Room-temperature parameter values were accurately determined: the quadrupole splitting (Q.S. = 0.541(6) mm·s$^{-1}$) is somewhat larger than that of ferrocenium (Q.S. = 0.2 mm·s$^{-1}$) and compares well to that of the ferric moiety of biferrocenium-type salts in the localized mixed-valence state.[31,32a] On the other hand, the isomer shift (I.S. = 0.515(3) mm·s$^{-1}$ *vs* Fe) is close to that of ferrocenium (I.S. = 0.43 mm·s$^{-1}$). The small Q.S. value[33] provides evidence for the $(a_1)^2(e_2)^3$ configuration of the 17-electron state as shown

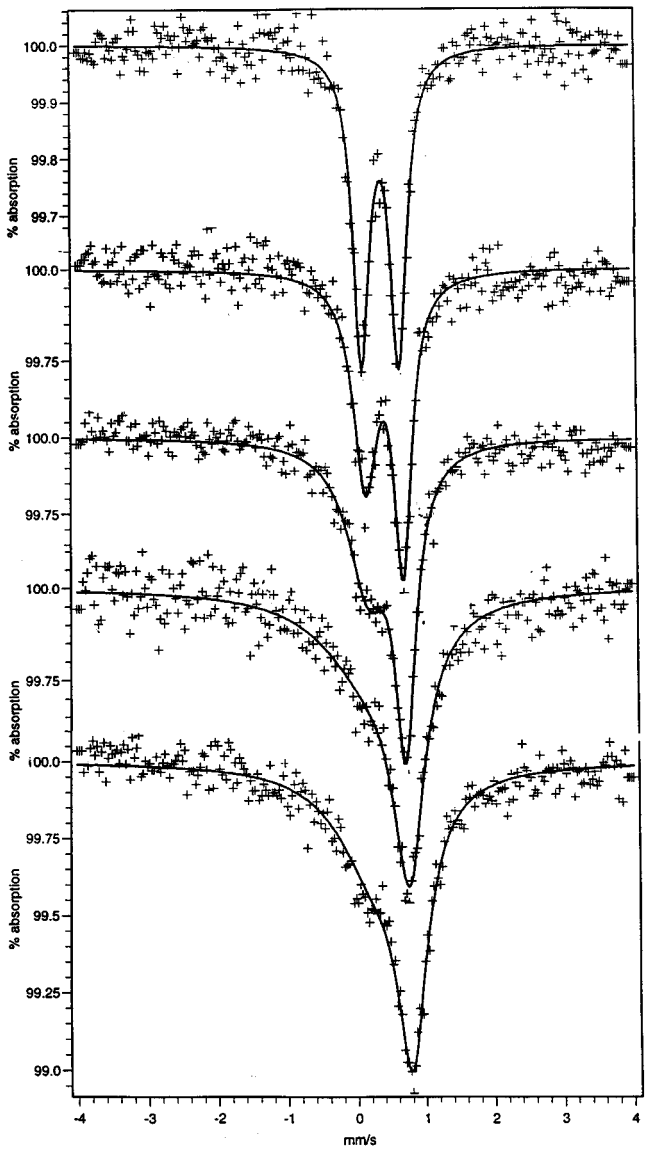


**Figure 3.** Mössbauer spectra, least-squares fitted with the symmetrical doublet of **1**[$SbCl_6$]$_2$ at room temperature (top) and the asymmetrical doublet at low temperature (bottom). Temperatures from top to bottom: 295, 180, 120, 80, and 4.2 K.

(26) (a) Richardson, D. E.; Taube, H. *Coord. Chem. Rev.* **1984**, *60*, 107. (b) Richardson, D. E.; Taube, H. *Inorg. Chem.* **1981**, *20*, 1278.

(27) Astruc, D. *Acc. Chem. Res.* **1986**, *19*, 377.

(28) (a) Liston, D. J.; Lee, Y. J.; Scheidt, W. R.; Reed, C. A. *J. Am. Chem. Soc.* **1989**, *111*, 6643. (b) Shelly, K.; Reed, C. A.; Lee, Y. J.; Scheidt, W. R. *J. Am. Chem. Soc.* **1986**, *108*, 3117. (c) This technique also provided a correct elemental analysis of **1**[$SbF_6$]$_2$ after extraction with MeCN. (d) Attempts to record X-ray crystal structures of members of the family **1**, **1**[$PF_6$] and **1**[$SbCl_6$]$_2$, failed because of disorder due to the fact that the Cp* and $C_6Me_6$ rings are so similar (unpublished work from K. N. Raymond's and L. Ouahab's groups in Berkeley and Rennes, respectively, whose attempts are gratefully acknowledged).

(29) Evans, D. F. *J. Chem. Soc.* **1959**, 2003.

(30) Fettouhi, M.; Ouahab, L.; Hagiwara, M.; Codjovi, E.; Kahn, O.; Constant-Machado, H.; Varret, F. *Inorg. Chem.* **1995**, *34*, 4152.

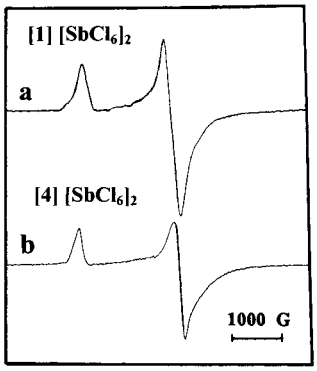


**Figure 4.** ESR spectra at 3.8 K of neat samples of (a) **1**$[SbCl_6]_2$ ($g_{||}$ = 3.5688 and $g_\perp$ = 1.8125) and (b) **4**$[SbCl_6]_2$ ($g_{||}$ = 3.625; $g_\perp$ = 1.739).

long ago in the case of unsubstituted ferrocenium,[32b] and as confirmed by our DFT calculations (vide infra). For roughly estimating the Q.S. value, we add up the contribution of the close shell (18-electron) and that of an electronic hole, depending on the nature of the unfilled orbital. Thus, the expected value is ca.|+2.5 (18e) + 3 or − 3| = 5.5 or 0.5 mm·s$^{-1}$ for the $(e_2)^4(a_1)^1$ or $(a_1)^2(e_2)^3$ configurations, respectively.[32a] The Q.S. value is not sensitive to the thermal population effect in the $e_2$ doublet, since the *xy* and $x^2-y^2$ orbitals provide identical contributions to the electric-field gradient tensor.[32b]

**ESR.** The ESR spectrum of a neat sample of **1**$[SbCl_6]_2$ was recorded at 3.8 K (Figure 4) and shows two *g* values: $g_{||}$ = 3.5688 and $g_\perp$ = 1.8125.

These values reflect the rhombic distortion due to the Jahn−Teller effect causing the splitting of the $x^2-y^2$ and *xy* orbitals which are degenerate in ferrocene and in $\mathbf{1}^+$ (vide infra). By using a simple adiabatic model, the *g* values lead, according to Prins,[33a] to the energy splitting $\Delta E$ of the degenerate $e_2$ orbitals (eq 1):

$$g_{||} = 2(1 - 2\lambda_0/\Delta E) \quad \text{with } \lambda_0 = -400 \text{ cm}^{-1} \qquad (1)$$

This equation leads to the splitting value $\Delta E = E(x^2-y^2) - E(xy)$ around 1000 cm$^{-1}$ for $\mathbf{1}^{2+}$, $\mathbf{2}^{2+}$, and $\mathbf{4}^{2+}$. By using the same model and equation, an almost identical value (900 cm$^{-1}$) was obtained for isoelectronic ferrocenium,[29a] but much larger values were calculated for unstable $[FeCp(polyaromatic)]^{2+}$ complexes.[19] Both $[FeCp(arene)]^{2+}$ and ferrocenium families are supposed to have the ground-state electronic structure $^2E_2$ corresponding to the $(a_1)^2(e_2)^3$ electron configuration (*vide infra*).[34b] However, for ferrocenium, other techniques gave different splittings: photoelectron spectroscopy yielded a value of 2800 cm$^{-1}$ [33b] while Raman spectroscopy[33c] and magnetic susceptibility[33d] gave a spliting of only 300 cm$^{-1}$ and model calculations led to 700 cm$^{-1}$.[33e] Finally, inelastic neutron scattering provided a value of 515 cm$^{-1}$.[33b] This later value took into account the vibronic mixing whereas previous data following the adiabatic model did not. Thus, it probably better represents the description of the actual splitting, which is very small. In any case, the Jahn−Teller coupling is weaker in $d^5$ than in $d^7$ metallocenes and metal-sandwich complexes. This is evidenced by the theoretical investigations of the various possible electron configurations which are analyzed below.

**Stability and Oxidation Chemistry of 1$[SbX_6]_2$ (X = Cl or F).** In the solid state, the salts of $\mathbf{1}^{2+}$ are stable in air for several hours. They are soluble in $SO_2$ and in MeCN and are rapidly reduced to yellow $\mathbf{1}^+$ by water in MeCN at −30 °C or by ferrocene in $CH_2Cl_2$. In particular, the reaction of **1**$[SbCl_6]_2$ with 1 equiv of ferrocene in $CH_2Cl_2$ at 20 °C quantitatively gave insoluble $[FeCp_2][SbCl_6]$ and soluble **1**$[SbCl_6]$. Unlike ferrocenium salts, the salts of $\mathbf{1}^{2+}$ are useful oxidants to remove one electron from complexes whose redox potentials are in the range of 0.4−1 V *vs* $[FeCp_2]^{0/+}$. The main known strong single-electron oxidants, their potentials, and an example of their use are gathered in Table 2 for comparison.

To avoid solvent problems (impurities rapidly reduce $\mathbf{1}^{2+}$ to $\mathbf{1}^+$ in a homogeneous solution), it is best to use $\mathbf{1}^{2+}$ salts as a suspension in the $CH_2Cl_2$ solution of the compound to oxidize. The reduced salt **1**$[SbCl_6]$ is soluble in $CH_2Cl_2$ whereas the oxidized product is insoluble, thus easy to separate. For instance, **1**$[SbCl_6]_2$ (neat) oxidized $[Ru(bipy)_3][PF_6]_2$ to the green 17-electron $Ru^{III}$ trication[34] in $CH_2Cl_2$.[35] Another example is the oxidation of the well-known cluster $[FeCp(\mu_3\text{-}CO)]_4$ [36a] to its mono- and dications. Oxidation of the neutral cluster to the monocation is relatively easy,[36b−d] but cannot be achieved with ferrocenium salts because the first oxidation potential of the cluster ($E_{1/2}$ = −0.04 V *vs* $[FeCp_2]^{+/0}$) is too close to that of ferrocene. Thus, **1**$[SbCl_6]_2$ quantitatively oxidizes the cluster to its monocation in $CH_2Cl_2$ at 20 °C. Other strong oxidants can also effect this oxidation[36b−d] (even $NO^+$) if they are not used in excess, because the monocationic cluster is relatively robust and the dicationic cluster is not. Although the second single-electron oxidation of the cluster is reversible at 0.6 V vs $[FeCp_2]^{0/+}$, all the reported attempts to isolate this dication were unsuccessful and yielded cationic mononuclear species resulting from the breakdown of the cluster framework.[36c,d] Reaction of the neutral cluster with 2 equiv of **1**$[SbCl_6]_2$ or of the monocationic cluster with 1 equiv of **1**$[SbCl_6]_2$ in dry $CH_2Cl_2$ yielded the dicationic cluster as a black-green precipitate in 90% yield in addition to soluble **1**$[SbCl_6]$. That the integrity of the cluster was retained was shown by reduction of the insoluble dicationic cluster by 2 equiv of $[FeCp^*_2]$ in $CH_2Cl_2$. The neutral cluster was obtained in 95% isolated yield in this way and was found pure with TLC and $^1H$ NMR and infrared spectroscopies after removal of $[FeCp^*_2][SbCl_6]$. These redox equations are summarized in Scheme 2.

(31) For further examples and more refined calculations, see: (a) Boukheddaden, K.; Linarès, J.; Bousseksou, A.; Nasser, J.; Rabah, H.; Varret, F. *Chem. Phys.* **1993**, *170*, 47. (b) Rabah, H.; Guillin, J.; Cérèze-Ducouret, A.; Grenèche, J. M.; Talham, D.; Boukheddaden, K.; Linarès, J.; Varret, F. *Hyperfine Interact.* **1993**, *77*, 51.

(32) (a) Hendrickson, D. N. In *Mixed Valence Systems: Applications in Chemistry, Physics and Biology*; Prassides, K., Ed.; NATO ASI Series; Kluwer: Dordretch, 1991; pp 7−28. (b) Collins, R. L. *J. Chem. Phys.* **1965**, *49*, 1072.

(33) (a) Prins, R. *Mol. Phys.* **1970**, *19*, 603. (b) Stebler, A.; Furrer, A.; Ammeter, J. A. *Inorg. Chem.* **1984**, *23*, 3493 and references therein; (c) Aleksanyan, V. T.; Haley, L. V.; Koningstein, J. A.; Parameswaran, T. *J. Chem. Phys.* **1977**, *66*, 3835. (d) Hendrickson, D. N.; Sohn, Y. S.; Gray, H. B. *Inorg. Chem.* **1971**, *10*, 1559. (e) Sohn, Y. S.; Hendrickson, D. N.; Gray, H. B. *J. Am. Chem. Soc.* **1970**, *92*, 3233; **1971**, *93*, 3603. Rabalais, J. W.; Werme, L. O.; Bergmark, T.; Karlsson, L.; Hussain, M.; Siegbahn, K. *J. Chem. Phys.* **1979,** *57*, 1185.

(34) $[Ru(bpy)_3]^{2+/3+}$, $E_{1/2}$ = 0.87 V vs $[FeCp_2]^{0/+}$ in MeCN: Templeton, J. L. *J. Am. Chem. Soc.* **1979**, *101*, 4906.

(35) $\mathbf{1}^{2+}$ can also oxidize the complexes $[Cr(arene)(CO)_3]$ to their 17-electron radical cations as indicated by the presence of new strong infrared bands, for instance at 1978 and 2050 cm$^{-1}$ for arene = $C_6Me_6$, analogous to those recently recorded by Sweigart et al. in their spectroelectrochemical study of the anodic oxidation of $[Cr(C_6Et_6)(CO)_3]$.[21b] More detailed studies of the electronic structure of these radical cations are underway.

(36) (a) King, R. B. *Inorg. Chem.* **1966**, *5*, 2227. (b) Greatrex, R.; Greenwood, N. N. *Discuss. Faraday Soc.* **1969**, *47*, 126. (c) Ferguson, J. A.; Meyer, T. J. *J. Chem. Soc. Chem. Commun.* **1971**, 623. (d) Wong, H.; Sedney, D.; Reiff, W. M.; Frankel, R. B.; Meyer, T. J.; Salmon, D. *Inorg. Chem.* **1978**, *17*, 194. (e) the thermal decomposition of the dicationic cluster over several days gives a known $[FeCp(CO)_3]^+$ salt: Román, E.; Astruc, D. *Inorg. Chem.* **1979**, *11*, 3284. (f) Further studies of the electronic structure of this dicationic 58-electron cluster will be reported later.

**Table 2.** Oxidations with Very Strong Single-Electron Oxidants ($E°$ Values Are Given *vs* $[FeCp_2]^{0/+}$)

| oxidant[a] | solvent | $E°$ (V) | example of oxidation | ref |
|---|---|---|---|---|
| $[O_2][EF_6]$(E = Pt, Sb, As) | | 4.9 (calc) | $C_6F_6$ (irrev) | 12a |
| $[N(C_6H_3Br_2\text{-}2,4)_3^{\bullet}][Y]$ | MeCN | 1.14 | $C_{76}$ | 16 |
| $[FeCp^*(C_6Me_6)]^{\bullet}[Y]_2$ | $CH_2Cl_2$ | 1.03 | $[FeCp(\mu_3\text{-}CO)]_4^{+}$ | this work |
| | MeCN | 0.925 | | this work |
| | $SO_2$ | 0.92 | | this work |
| $[NO][BF_4]$ | $CH_2Cl_2$ | 1.00 | $N(C_6H_4Br\text{-}4)_3$ | 8a |
| | MeCN | 0.87 | | 8a |
| $[Ce^{IV}][NH_4]_2[NO_3]_6$ | 1 M $H_2SO_4$ | 0.80 | $[OsCp_2]$ (irrev) | 6 |
| | $H_2O$ | 0.88 | | 54 |
| [thianthrene$^{\bullet}$] $[BF_4]$ | MeCN | 0.86 | $[HgR_2]$ (irrev) | 55 |
| $[N(C_6H_4Br{-}4)_3^{\bullet}][BF_4]$ | $CH_2Cl_2$ | 0.70 | $[Fe(CO)_3(PPh_3)_2]$ | 56 |
| | MeCN | 0.67 | | 56 |
| $[Fe(bpy)_3^{\bullet}][BF_4]_3$ | MeCN | 0.66 | metal hydrides | 5 |
| | $CH_2Cl_2$ | 0.65 | | 5 |
| $[Ag][BF_4]$ | $CH_2Cl_2$ | 0.65 | $[Cr(CNC_6H_4Me\text{-}4)_6]^{2+}$ | 57 |

[a] [Y] = $[SbCl_6]$.

**Scheme 2**

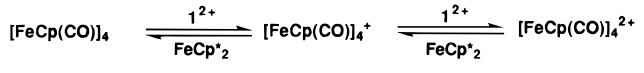


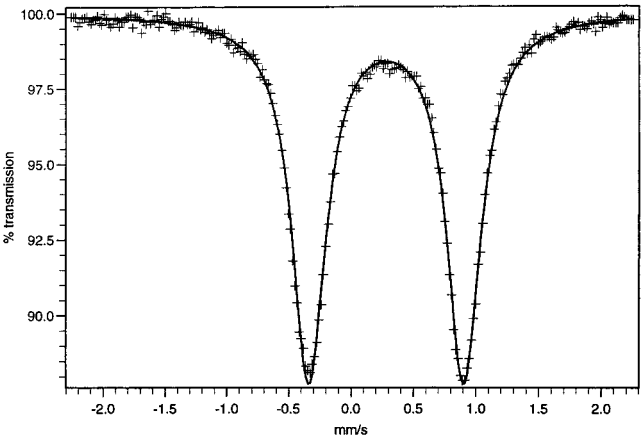


**Figure 5.** Mössbauer spectra, least-squares fitted, of $[FeCp(CO)]_4$-$[SbCl_6]_2$ at 4.2 K under zero field.

The $[SbCl_6]^-$ salt of the dicationic cluster showed new infrared bands at $\nu_{CO}$ = 1735 and 1780 $cm^{-1}$ as expected ($\nu_{CO}$ = 1620 and 1700 $cm^{-1}$ in the neutral and monocationic clusters, respectively).[36b,c] As an indication of the instability of the dicationic cluster in air,[36d] these new CO bands weakened upon exposure to air, disappearing after 2 h. The zero-field Mössbauer spectra of the dicationic cluster were recorded at 4,77, and 293 K and showed a single temperature-independent sharp doublet without iron impurities (Figure 5).

The Mössbauer sample was checked by infrared spectra (vide supra) before and after recording the Mössbauer spectra. The Mössbauer parameters (I.S. = 0.405(1) mm·$s^{-1}$; Q.S. = 1.224-(1) mm·$s^{-1}$ vs iron) are relatively close to, although significatively different from, those of the previously reported spectra of the neutral cluster (I.S. = 0.66 mm·$s^{-1}$; Q.S. = 1.76 mm·$s^{-1}$) and the monocationic cluster (I.S. = 0.67 mm·$s^{-1}$; Q.S. = 1.40 mm·$s^{-1}$).[36a] The lack of large variation of the Mössbauer parameters upon single-electron oxidation of the neutral cluster to the monocation was interpretated in terms of removal of electron density from the ligands rather than from the tetrametallic cluster framework.[36a] This explanation also essentially applies to the dicationic cluster although a moderate lowering of the I.S. value is now observed in the second oxidation whereas there was none in the first one.[36e]

Finally, $[FeCp(C_6Me_6)][PF_6]$ can be used as a redox catalyst for anodic oxidations even if the dicationic oxidized form involved in the redox-catalytic process is not isolated, since the anodic oxidation of $[FeCp(C_6Me_6)][PF_6]$ is fully reversible in $SO_2$. For instance, $[FeCp(C_6Me_6)][PF_6]$ catalyzes the useful ring-opening anodic oxidation of furfural[37] in $SO_2$ solution at −40 °C on Pt when the anodic potential is set at the potential of the $Fe^{II}/Fe^{III}$ redox system, the overpotential being 0.7 V. The rate constant for the oxidation of furfural under these conditions by electrogenerated $[FeCp(C_6Me_6)]^{2+}$ is $k$ = 115 mol·$L^{-1}$·$s^{-1}$ as determined by cyclic voltammetry with Nicholson and Shain's equation[37b] from the enhancement of the intensity of the oxidation wave of $[FeCp(C_6Me_6)][PF_6]$ in the presence of furfural.

**Synthesis, Characterization, and Stability of $2[SbX_6]_2$ and $4[SbX_6]_2$ (X = Cl or F).** Oxidation of **2**$[PF_6]$ in $CH_2Cl_2$ at 20 °C by $SbCl_5$ is slower than that of **1**$[PF_6]$ and needs about a minute to reach completion. The purple-brown precipitate was purified as indicated above for **1**$[SbCl_6]_2$, which yielded 70% of purple **2**$[SbCl_6]_2$. Using $SbF_5$ in $SO_2$ at −40 °C also required about a minute for complete color change from light yellow to deep purple. The complexes **2**$[SbCl_6]_2$ and **2**$[SbF_6]_2$ are stable in the solid state (ESR spectrum of **2**$[SbCl_6]_2$ at 4 K: $g_{||}$ = 3.569; $g_{\perp}$ = 1.789) and gave satisfactory elemental analyses. They were reduced more quickly than the $\mathbf{1}^{2+}$ salts in air. The same reactions with $[FeCp(durene)][PF_6]$, **4**$[PF_6]$, were even slower and required 0.5 h. The reaction with $SbCl_5$ gave a brown powder which, despite multiple washing with $CH_2Cl_2$, did not yield colorless $CH_2Cl_2$ or the same very purple color of the solid as for the $\mathbf{1}^{2+}$ and $\mathbf{2}^{2+}$ salts. Nevertheless, from this orange-purple solid (10% of the reaction product after washing), a good ESR spectrum was recorded, similar to those of **1**$[SbCl_6]_2$ and **2**$[SbCl_6]_2$ ($g_{||}$ = 3.625; $g_{\perp}$ = 1.739, Figure 5b), indicating the presence of **4**$[SbCl_6]_2$. The reaction was also very slow with $SbF_5$ in $SO_2$ (0.5 h at −10 °C; no reaction at −40 °C).

**Effective Oxidizing Power of $SbCl_5$ in $CH_2Cl_2$ and $SbF_5$ in $SO_2$.** The same reaction of $[FeCp^*(arene)][PF_6]$ complexes with a number of Me substituents lower than four never gave a color change indicative of the electron-transfer reaction with either $SbCl_5$ in $CH_2Cl_2$ at 20 °C or $SbF_5$ in $SO_2$ at −10 °C. Thus, since the oxidation of these salts is fully reversible in $SO_2$ and since we know that the shift of $E_{1/2}$ induced by each methyl substituent in $SO_2$ is 60 mV (Table 1), it appears that this series of reactions gives a relatively accurate indication of the oxidizing power of $SbCl_5$ in $CH_2Cl_2$ at 20 °C and of $SbF_5$

(37) (a) Tanaka, H.; Kobayasi, Y.; Torii S. *J. Org. Chem.* **1976**, *41*, 3482. (b) Nicholson, R. S.; Shain, I. *Anal. Chem.* **1964**, *36*, 706.

**Chart 2**

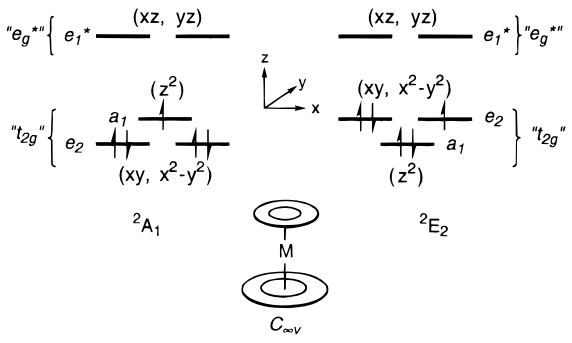


in $SO_2$ at −40 to −10 °C.[38] The reduction of $SbCl_5$ and $SbF_5$ is totally irreversible, and therefore it is difficult to determine their standard redox potentials. The effective oxidation potential of these strong oxidants is very much dependent on the rate of the follow-up reaction. The borderline is the oxidation potential of **4**$[PF_6]$, 1.01 V vs $[FeCp_2]^{0/+}$ in $SO_2$. The oxidizing power of $SbF_5$ at −10 °C in $SO_2$ is not larger than that of $SbCl_5$ in $CH_2Cl_2$ at 20 °C.[2] It is known that $SbF_5$ is a better oxidant than $SbCl_5$,[2a] but the solvent and temperature of reaction are also important in this matter, since they influence the rates of the follow-up reactions of the $SbCl_5$ and $SbF_5$ compounds after electron transfer.[38]

**Theoretical Investigations of the Electronic Structure of $[FeCp(C_6H_6)]^{2+}$ and Related 17-Electron Complexes.** We describe below a detailed DFT analysis of the electronic structure of the 17e title compounds which has been carried out to provide a general rationalization of the electrochemical and spectroscopic behavior of the 17e title compounds. In addition, these calculations allow accurate prediction of the molecular structures of these species which could not be obtained so far with ordinary X-ray techniques. A detailed comparison with 18e parent complexes as well as with the related 17e $[FeCp_2]^+$ and $[Fe(C_6H_6)_2]^{3+}$ provides a full understanding of the effect of oxidation on metallocenes.

**Qualitative Considerations and Description of the Problem.** The qualitative electronic structure of a transition-metal sandwich complex is easily understood by taking advantage first of the pseudooctahedral environment of the metal and second the overall pseudocylindrical symmetry ($D_{\infty h}$ or $C_{\infty v}$) of the molecule. The pseudooctahedral ligand field splits the valence metallic d-shell into two well-energy-separated groups of orbitals: the antibonding "$e_g$*" set and the nonbonding "$t_{2g}$" group. In the pseudo-$C_{\infty v}$ molecular symmetry, the former, of dominant *xz* and *yz* character, is labeled[39] $e_1$* and the latter splits into two closely spaced $a_1$ and $e_2$ levels (see Chart 2). In a 17-electron ($d^5$) sandwhich complex, the hole is expected to be located either in the $a_1$ ($z^2$) or in the $e_2$ ($x^2-y^2$, *xy*) levels, leading to two possible ground-state configurations: $^2A_1$ and $^2E_2$. One may be tempted to predict that the 17-electron ground state corresponds to the creation of a hole in the HOMO of its 18-electron parent. However, because the $a_1$ and $e_2$ levels are often rather close in energy, the electronic/geometric relaxation that occurs upon removal of one electron can induce a crossing between these two levels. From this point of view, the energy change of the $e_2$ level upon oxidation is expected to be larger since the $x^2-y^2$ and *xy* orbitals are somewhat mixed in a bonding fashion with the $\pi$* orbitals or the cyclic ligands, while the $a_1$ level is expected to have a smaller bonding character through some hybridization with the metal s valence orbital.[40] A Jahn−Teller splitting of the $e_2$ level is also expected in the case of the $(e_2)^3(a_1)^2$ configuration. Clearly, the question of the ground state of the 17-electron title compounds cannot be answered on qualitative grounds. DFT has recently proven to be an invaluable method for the determination of electronic structures of open-shell organometallic complexes.[41] For these reasons, we have undertaken DFT calculations on $[FeCp(C_6H_6)]^{2+}$ and some related compounds. In addition, DFT calculations would also allow the first structural determination for such a species, since there is no experimental crystal structure reported so far. For the sake of comparison, we have also carried out similar calculations on the ferrocenium cation for which more experimental data are avalaible.[42a] To complete the series of the Cp and/or benzene 17-electron sandwich species, the hypothetical $[Fe(C_6H_6)_2]^{3+}$ isoelectronic compound was also calculated. The three 18-electron parents were included in the calculations. The major energetic and metrical data of the various optimized models are reported in Tables 3−6 and in Figure 6.

**The $[FeCp_2]^{0/+}$ System.** The optimized $C_{5v}$ geometry of ferrocene is not significantly different from the eclipsed $D_{5h}$ conformation (see Computational Details). The calculated geometry (Table 3) is very close to that obtained previously by related DFT calculations.[42b,c] A satisfactory agreement is also obtained with previous ab initio results.[43] The computed Fe−C distances are only ≈0.02 Å longer than the experimental ones.[44] The theoretical and experimental C−C distances are not significantly different. The $e_2$ ($x^2-y^2$, *xy*) level of ferrocene lies significantly above the $a_1$ ($z^2$) level (0.32 eV). Consistently, the $^2E_2$ state of ferrocenium is more stable than the $^2A_1$ state by a value of the same order of magnitude (0.46 eV). This energy separation is of the same order of magnitude as proposed from PES experiments (0.54 eV).[33f] In the considered $C_{2v}$ eclipsed conformation of the $(e_2)^3(a_1)^2$ configuration (see Computational Details), the $^2E_2$ states split into $^2A_1$ and $^2B_2$, depending on the hole being in the component of the $e_2$ level which is symmetrical or antisymmetrical with respect to the plane bissecting the two rings. These two states can be considered as being degenerate, their computed energy difference (0.006 eV) being insignificant. The corresponding adiabatic ionization potential (IP) given in Table 3 is in satisfying agreement with that found by PES experiments (6.72 eV).[33f] The $^2E_2$ and $^2A_1$ optimized geometries of $[FeCp_2]^+$ exhibit Fe−C distances which are slightly longer than those in $[FeCp_2]$, in agreement with the weak bonding character of the $e_2$ and $a_1$ orbitals. The weaker bonding character of the $a_1$ orbital is consistent with the less pronounced Fe−C bond lengthening in the $^2A_1$ state (Table 3). The two $^2E_2$ geometries are shown in

(38) An additionnal driving force of 0.1 to 0.2 V must be considered for the reaction with $SbCl_5$ because the $\mathbf{1}^{2+}$ salt formed precipitates. This is not the case with $SbF_5$.

(39) Throughout this paper we use, as usually done for metal-sandwhich complexes, the notations $e_1$, $a_1$, and $e_2$ rather than $\pi$, $\sigma$, and $\delta$ for labeling the $C_{\infty v}$ irreducible representations.

(40) Albright, T. A.; Burdett, J. K.; Whangbo, M.-H. *Orbital Interactions in Chemistry*; Wiley: New York, 1985.

(41) (a) Braden, D. A.; Tyler, D. R. *J. Am. Chem. Soc.* **1998**, *120*, 942. (b) Legzdins, P.; McNeil, S.; Smth, K. M.; Poli, R. *Organometallics* **1998**, *17*, 615. (c) Cacelli, I.; Keogh, D. W.; Poli, R.; Rizzo, A. *New J. Chem.* **1997**, *21*, 133. (d) Ricca, A.; Bauschlicher, C. W. *J. Phys. Chem.* **1995**, *99*, 5922.

(42) (a) Landers, A. G.; Lynch, M. W.; Raaberg, S. B.; Rheingold, A. L.; Lewis, J. E.; Mammano, N. J.; Zalkin, A. *J. Chem. Soc. Chem. Com.* **1976**, 931. (b) Fan, L.; Ziegler, T. *J. Chem. Phys.* **1991**, *95*, 7401. (c) Bérces, A.; Ziegler, T.; Fan, L. *J. Phys. Chem.* **1994**, *98*, 1584.

(43) (a) Park, C.; Almlöf, J. *J. Chem. Phys.* **1991**, *95*, 1829. (b) McKee, M. L. *J. Am. Chem. Soc.* **1993**, *115*, 2818.

(44) (a) Haaland, A. *Top. Curr. Chem.* **1975**, *53*, 1. (b) Haaland, A. *Acc. Chem. Res.* **1979**, *12*, 415. (c) Seiler, P.; Dunitz, J. D. *Acta Crystallogr.* **1979**, *B35*, 2020.

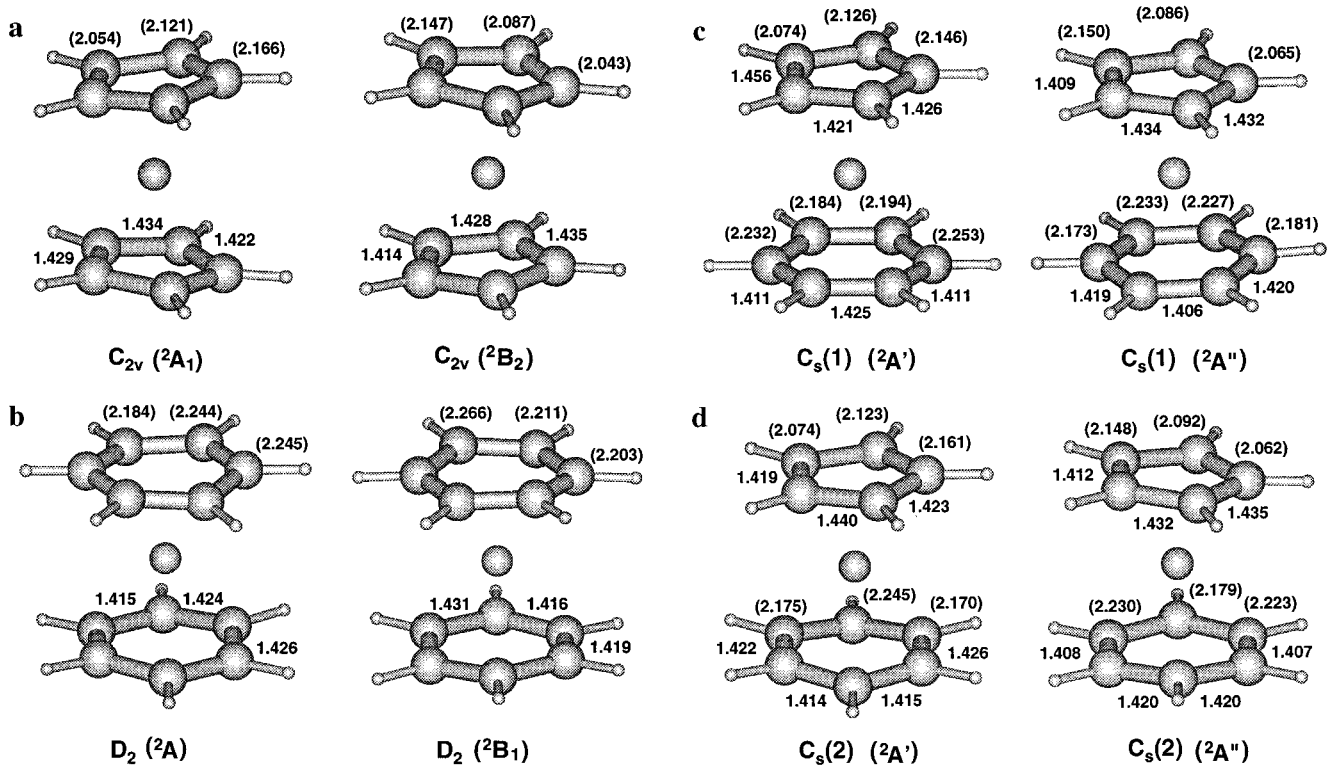


**Figure 6.** Optimized geometries corresponding to the $^2E_2$ state (see text) of **(a)** $[FeCp_2]^+$, (b**)** $[Fe(C_6H_6)_2]^{3+}$, (c**)** $[FeCp(C_6H_6)]^{2+}$ (Cs(1) conformation), and (d**)** $[FeCp(C_6H_6)]^{2+}$ (Cs(2) conformation).

**Table 3.** Major Averaged Optimized Bond Distances (Å) of $[FeCp_2]$and $[FeCp_2]^+$ and Relative Energies (eV) of the Lowest States of the 17-Electron Cation

| | $Fe(Cp)_2$ | $[FeCp_2]^+$ | | |
|---|---|---|---|---|
| electronic state[a] | $^1A_1$ ($^1A_1$) | $^2A_1$ ($^2A_1$) | $^2A_1$ ($^2E_2$) | $^2B_2$($^2E_2$) |
| sym constraint during geometry optimization | $C_{5v}$[b] | $C_{5v}$[b] | $C_{2v}$ | $C_{2v}$ |
| Fe−C | 2.048 | 2.075 | 2.104 | 2.102 |
| C−C | 1.434 | 1.435 | 1.428 | 1.428 |
| C−H | 1.090 | 1.091 | 1.091 | 1.091 |
| rel energy (eV) | 7.11[c] | 0.46 | 0.01 | 0.00 |

[a] Labels in parentheses assume the $C_{\infty v}$ pseudosymmetry. [b] No significant departure away from $D_{5h}$ symmetry. [c] Adiabatic ionization potential.

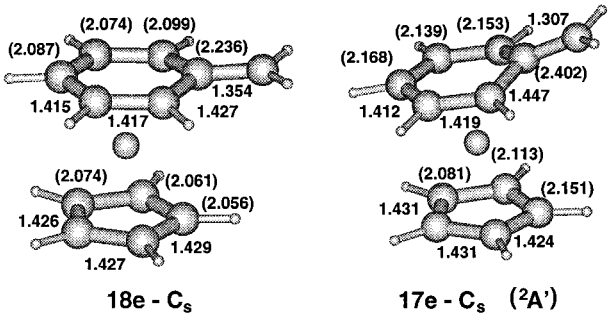


**Figure 7.** Ground-state optimized geometries of $[FeCp(C_6H_5NH_2)]^+$ and $[FeCp(C_6H_5NH_2)]^{2+}$.

Figure 8a. They are close to $C_{2v}$ symmetry, and the slight nonequivalence of the two Cp rings is probably not significance at the considered level of theory. The rings are somewhat distorted away from the axial symmetry, leading to a dispersion of the Fe−C bond distances. The *quasi*-degenerate $^2A_1$ and $^2B_2$ states lead to different distortions, consistent with the different nodal properties of the singly occupied $e_2$ orbitals ($a_1$ or $b_2$), which are bonding combinations between the $x^2-y^2$ or $xy$ orbitals and the proper $a_1$ or $b_2$ component of the $\pi^*$(Cp) orbitals.

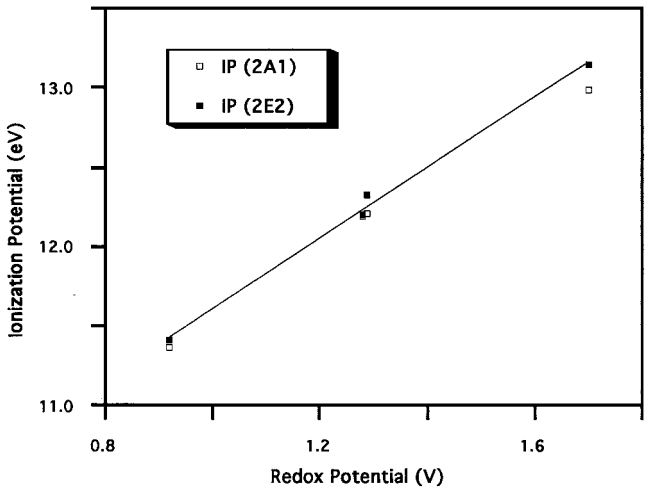


**Figure 8.** Ionization potentials of $[FeCp(C_6H_6)]^+$, $[FeCp(C_6Me_6)]^+$, $[FeCp^*(C_6H_6)]^+$, and $[FeCp^*(C_6Me_6)]^+$computed by the Slater transition-state method at the NLDA level vs redox potentials ($E_{1/2}$ vs $[FeCp_2]$ in $SO_2$). The linear fit curve corresponds to the $^2E_2$ ionization potential.

Our results on ferrocenium are in agreement with magnetic, EPR, and PES studies on decamethylferrocenium and other $MCp_2$ 17-electron complexes which found the same $^2E_2$ ground-state configuration.[33,45] This is also in agreement with the X-ray experimental structures of ferrocenium and derivatives[46] which indicate significant lengthening of Fe−C bonds when going

(45) Robbins, D. L.; Edelstein, N.; Spencer, B.; Smart, J. C. *J. Am. Chem. Soc.* **1982**, *104*, 1982 and references therein.

(46) (a) Landers A. G.; Lynch, M. W.; Raaberg, S. B.; Rheingold, A. L.; Lewis, J. E. *J. Chem. Soc. Chem. Commun.* **1976**, 931. (b) Gohlen, S. Ph.D. Thesis, University of Rennes 1, 1997.

**Table 4.** Major Averaged Optimized Bond Distances (Å) of $[Fe(C_6H_6)_2]^{2+}$and $[Fe(C_6H_6)_2]^{3+}$and Relative Energies (eV) of the Lowest States of the 17-Electron Trication

| | $[Fe(C_6H_6)_2]^{2+}$ | $[Fe(C_6H_6)_2]^{3+}$ | | |
|---|---|---|---|---|
| electronic state[a] | $^1A_1$ ($^1A_1$) | $^2A_1$ ($^2A_1$) | $^2A_1$ ($^2E_2$) | $^2B_2$ ($^2E_2$) |
| sym constraint during geometry optimization | $C_{6v}$[b] | $C_{6v}$[b] | $D_2$ | $D_2$ |
| Fe−C | 2.124 | 2.167 | 2.229 | 2.197 |
| C−C | 1.417 | 1.426 | 1.422 | 1.422 |
| C−H | 1.095 | 1.101 | 1.100 | 1.101 |
| rel energy (eV) | 17.70[c] | 0.20 | 0.02 | 0.00 |

[a] Labels in parentheses assume the $C_{\infty v}$ pseudosymmetry. [b] No significant departure away from $D_{6d}$ symmetry. [c] Adiabatic ionization potential.

**Chart 3**

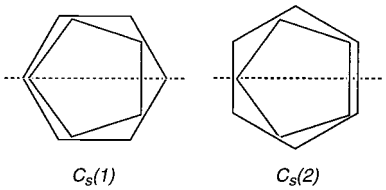


from ferrocene to ferrocenium. These results gave us confidence for undertaking the study on the bis-benzene and cyclopentadienyl−benzene systems.

**The $[Fe(C_6H_6)_2]^{2+/3+}$ System.** The calculations on these species have been made assuming the staggered conformation (see Computational Details). The major results are given in Table 4. In contrast to ferrocene, the $e_2$ level of the 18-electron $[Fe(C_6H_6)_2]^{2+}$ model is situated below the $a_1$ level (by 0.12 eV). This is due to the better $\pi$-acceptor ability of the benzene rings which tends to stabilize more importantly the $e_2$ level, as compared to the cyclopentadienyl anions. As for the bis-cyclopentadienyl parents, the removal of one of the $e_2$ electrons in $[FeCp(C_6H_6)]^{2+}$ is expected to produce a more pronounced distortion away from the axial symmetry than the removal of an $a_1$ electron. This is exemplified in Figure 8b, which shows the $^2A$ and $^2B_1$ optimized geometries of $[Fe(C_6H_6)_2]^{3+}$. As for the corresponding electron configurations in ferrocenium, they are *quasi*-degenerate and exhibit different dispersion of the Fe−C bond distances which are consistent with the different nodal properties of the singly occupied $e_2$ bonding MO's. Due to the larger Fe−C bonding character of the $e_2$ level in the bis-(benzene) series, this distortion tends to provide a better stability for the $^2E_2$ states, despite the fact that the $a_1$ level is the HOMO of the 18-electron parent. The computed energy difference between the $^1A_1$ and $^2E_2$ states of $[Fe(C_6H_6)_2]^{3+}$ is smaller than in the case of $[FeCp_2]^{+}$.

**The $[FeCp(C_6H_6)]^{+/2+}$ System.** The highest possible symmetry for these species is $C_s$. Chart 3 shows the two $C_s$ conformations which can be considered, namely $C_s(1)$ and $C_s(2)$.

Calculations on the 18-electron $[FeCp(C_6H_6)]^{+}$ complex lead to a very close-to-perfect $C_{\infty v}$ symmetry, with almost rigorous degeneracy of the $e_1$ and the $e_2$ levels, and a rotational barrier not significantly different from zero (0.002 eV). The HOMO is the $a_1$ orbital, lying 0.10 eV above the $e_2$ level. The $a_1$ HOMO has less than 2% carbon participation. As expected, the $e_2$ orbitals have a more covalent character with localizations of 76%, 5%, and 13% on Fe, the $C_5$ ring, and the $C_6$ ring, respectively. The optimized geometry (Table 5) is in fairly good agreement with the experimental X-ray structure of the related $[FeCp(C_6Et_6)]^{+}$ cation.[47] The calculated level ordering and charge distribution of the 18-electron species are comparable to those obtained previously by Le Beuze et al. using Xα calculations on a frozen idealized geometry.[48] The $^2A_1$ state of the $C_s(1)$ conformation of the 17-electron $[FeCp(C_6H_6)]^{2+}$ complex is also very close to the ideal $C_{\infty v}$ symmetry. We were unable, however, to reach convergence for the $^2A_1$ state of the $C_s(2)$ conformation. As for $[FeCp_2]^{+}$ and $[Fe(C_6H_6)_2]^{3+}$, the $^2E_2$ state splits in the considered $C_s(1)$ and $C_s(2)$ geometries into two nearly degenerate states, $^2A'$ and $^2A''$, depending on the a′ or a″ nature of the singly occupied component of the $e_2$ HOMO. The very small splitting of the $^2E_2$ state in the three computed 17e complexes is closer to the value evaluated from neutron scattering (515 $cm^{-1}$)[33b] than the one proposed from ESR data with Prins' equation (ca. 1000 $cm^{-1}$)[33a] (*vide supra*). This latter value is actually in better agreement with the energy difference between the $^1A_1$ and $^2E_2$ states. Four different distortions away from the axial symmetry are obtained, depending on the $C_s(1)$ or $C_s(2)$ conformation and the $^2A'$ or $^2A''$ states (Figures 8c and 8d). They are all consistent with the nodal properties of the singly occupied HOMO. As expected from the largest benzene contribution of the $e_2$ level, the dispersion of the Fe−C($C_6H_6$) distances is more pronounced than that of the Fe−C(Cp) distances and the average [Fe−C($C_6H_6$)] distance is larger than the average Fe−C(Cp) distance. The four computed geometries are very close in energy, the lowest energy corresponding to the $^2A'$ state of the $C_s(1)$ conformation (Table 5). As expected from the largest benzene contribution to the $e_2$ level as compared to the $a_1$ orbital, the oxidation of $[FeCp(C_6H_6)]^{+}$ into the $^2A_1$ state of $[FeCp(C_6H_6)]^{2+}$ leads to a smaller lengthening of the Fe−ligand distances than that corresponding to the $^2E_2$ state.

**The $[FeCp(C_6H_5NH_2)]^{+/2+}$ System.** To check the above-mentioned electronic effect induced by the presence of a $NR_2$ group on the arene ligand we have also carried out the geometry optimization of the $[FeCp(C_6H_5NH_2)]^{+/2+}$system, assuming $C_s$ symmetry. In these species, the $\pi$-donor effect of the nitrogen lone pair significantly breaks the $C_{\infty v}$ pseudosymmetry and splits the $e_2$ level into two well-energy-separated a′ and a″ orbitals. The a′ component is a bonding combination of the $x^2-y^2$ orbital with the lowest unoccupied $\pi^*$ orbital of free aniline. Its larger Fe−C(arene) bonding character corresponds to the *ipso* carbon. This orbital is the HOMO of the 18-electron species. It has a participation of 69%, 12%, and 7% on Fe, N, and the $C_6$ ring, respectively. The ground state of the 17-electron species corresponds to one electron removed from this orbital. However, significant reorganization occurs upon oxidation, as illustrated in Figure 7, which shows the optimized geometries of the ground states of $[FeCp(C_6H_5NH_2)]^{+}$ and $[FeCp(C_6H_5NH_2)]^{2+}$.

The Fe−C(*ipso)* distance, already quite long in the 18-electron complex (2.236 Å), is significantly longer in the 17-electron complex (2.403 Å), due to the loss of Fe−C(*ipso)* bonding character upon oxidation. This elongation is associated with some bending of the ring and a shortening of the C−N bond. Obviously, the partial depopulation of the Fe−C(*ipso)* bonding HOMO of $[FeCp(C_6H_5NH_2)]^{+}$ leads to a close-to-$\eta^5$ Fe−arene bonding mode, indicating a significant participation of the iminium resonnant formula of Chart 1. The oxidation also significantly changes the HOMO localization. Its participation on Fe, N, and the $C_6$ ring is now 36%, 18%, and 23%. The computed adiabatic IP is 11.69 eV, a value 0.82 eV lower than that found for $[FeCp(C_6H_6)]^{+}$. This is in full agreement with

(47) Hamon, J.-R.; Saillard, J.-Y.; Le Beuze, A.; McGlinchey, M. J.; Astruc, D. *J. Am. Chem. Soc.* **1982**, *104*, 7459.

(48) Le Beuze, A.; Lissilliour, R.; Weber, J. *Organometallics* **1993**, *12*, 47.

**Table 5.** Major Averaged Optimized Bond Distances (Å) of $[FeCp(C_6H_6)]^+$ and $[FeCp(C_6H_6)]^{2+}$ and Relative Energies (eV) of the Lowest States of the 17-Electron Dication

| | $[FeCp(C_6H_6)]^+$ | $[FeCp(C_6H_6)]^{2+}$ | | | | |
|---|---|---|---|---|---|---|
| electronic state[a] | $^1A'$ ($^1A_1$) | $^2A'$ ($^2A_1$) | $^2A'$ ($^2E_2$) | $^2A''$ ($^2E_2$) | $^2A'$ ($^2E_2$) | $^2A''$($^2E_2$) |
| sym constraint during geometry optimization | $C_s$[b] | $C_s(1)$ | $C_s(1)$ | $C_s(1)$ | $C_s(2)$ | $C_s(2)$ |
| Fe−C(Cp) | 2.066 | 2.080 | 2.109 | 2.107 | 2.111 | 2.109 |
| C(Cp)−C(Cp) | 1.428 | 1.434 | 1.430 | 1.428 | 1.429 | 1.431 |
| C(Cp)−H | 1.093 | 1.093 | 1.095 | 1.096 | 1.096 | 1.095 |
| Fe−C($C_6H_6$) | 2.096 | 2.142 | 2.204 | 2.212 | 2.197 | 2.211 |
| C($C_6H_6$)−C($C_6H_6$) | 1.415 | 1.420 | 1.416 | 1.415 | 1.418 | 1.416 |
| C($C_6H_6$)−H | 1.093 | 1.095 | 1.096 | 1.096 | 1.097 | 1.097 |
| rel energy (eV) | 12.51[c] | 0.34 | 0.00 | 0.02 | 0.03 | 0.02 |

[a] Labels in parentheses assume the $C_{\infty v}$ pseudosymmetry. [b] In the case of the 18-electron species (left column), the $C_s(1)$ and $C_s(2)$ conformations lead to averaged bond distances which differ by less than 0.001 Å. [c] Adiabatic ionization potential.

**Table 6.** Selected Averaged Bond Distances (Å)[a] and Ionization Potentials (eV)[b] Computed for the $[Fe(C_5R_5)(C_6R'_6)]^+$ (R, R′ = H, Me) Series

| | Fe−C($C_5R_5$) | Fe−C($C_6R'_6$) | IP($^2A_1$) | IP($^2E_2$) |
|---|---|---|---|---|
| $[(C_5H_5)Fe(C_6H_6)]^+$ | 2.015 | 2.041 | 12.98 | 13.15 |
| $[(C_5Me_5)Fe(C_6H_6)]^+$ | 2.004 | 2.039 | 12.20 | 12.32 |
| $[(C_5H_5)Fe(C_6Me_6)]^+$ | 2.016 | 2.039 | 12.19 | 12.19 |
| $[(C_5Me_5)Fe(C_6Me_6)]^+$ | 2.017 | 2.062 | 11.36 | 11.41 |

[a] Geometries optimized at the LDA level. [b] The ionization potentials have been calculated at the LDA level on the NLDA-optimized geometries by using the transition state method and assuming either the $^2A_1$ or $^2E_2$ state for the oxidized species.

the difference between the oxidation potentials of the aniline complexes and that of the other $[FeCp(arene)]^+$ complexes (Table 1).

**Ionization Potentials (IP's) of $[Fe(C_5R_5)(C_6R'_6)]^+$ (R, R′ = H, Me).** Ionization potentials are directly related to redox potentials. The Slater transition state method[49] allows calculations of IP's at a reasonable computational cost. This method has been utilized to determine the IP's of $[FeCp(C_6H_6)]^+$, $[FeCp(C_6Me_6)]^+$, $[FeCp^*(C_6H_6)]^+$, and $[FeCp^*(C_6Me_6)]^+$ at the NLDA level. The considered geometries were those optimized at the NLDA level for the 18-electron species (see Computational Details). The corresponding Fe−C bond distances are reported in Table 6. As expected, the $[FeCp(C_6H_6)]^+$ values are slightly shorter than that optimized at the NLDA level (compare Tables 5 and 6). For each compound, two IP's were computed, depending on the considered $^2A_1$ or $^2E_2$ state of the oxidized form. These values are given in Table 6. Because they do not take into account the geometry relaxation of the oxidized form, these vertical IP's are expected to differ slightly from the energy difference between the optimized 18- and 17-electron species. In particular, the $^2E_2$ vertical IP's are expected to be somewhat larger, because of the significant ligand participation to the $e_2$ orbitals. Indeed, this latter value is equal to 13.15 eV for the $^2E_2$ state of $[FeCp(C_6H_6)]^{2+}$, as compared to 12.51 eV found for the energy difference between the fully optimized 18- and 17-electron species. This is the main reason the $^2A_1$ vertical IP is found to be lower than the $^2E_2$ one in these calculations. Ligand alkylation is expected to increase its $\pi$-donating capability, *i.e.* enhancing the destabilization of its $\pi$ bonding levels. As a result, the occupied $\pi$ bonding $e_1$ ligand orbitals interact more strongly with the metallic $e_1$ vacant orbitals, leading to a stronger bonding interaction with the alkylated ring. This effect is sketched in Chart 4 in the case of Cp alkylation. It should be the major one responsible for the variation in bond strength. Since the cyclopentadienyl anion is a better donor ligand than benzene, this effect is expected to be stronger in the case of Cp alkylation. On the other side,

(49) Slater, J. C. *Adv. Quantum Chem.* **1972**, *6*, 1.

**Chart 4**

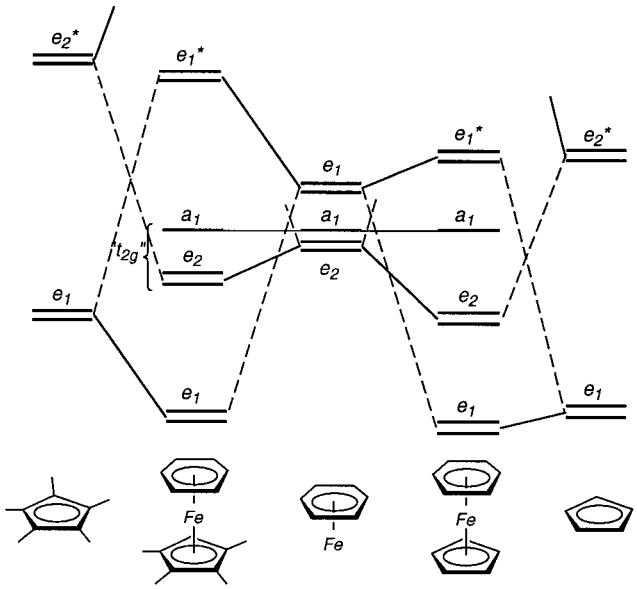


alkylation reduces the ligand $\pi$-accepting ability, i.e. enhancing the destabilization of its $\pi^*$ antibonding levels. As a result, the interaction of the ligand $\pi^*$ ($e_2$) orbitals with the metallic $e_2$ orbitals is weaker, as sketched in Chart 4 in the case of Cp alkylation. Within the "$t_{2g}$" block, the $a_1$ orbital is expected to be less perturbed than the $e_2$ level because of its larger nonbonding character. These qualitative predictions are reproduced by the calculations on the $[Fe(C_5R_5)(C_6R'_6)]^+$ (R, R′ = H, Me) series. Indeed, one can see in Table 6 that the methylation of one of the rings leads to the shortening of the corresponding Fe−C distances, this shortening being really significant only in the case of the pentamethylcyclopentadienyl species. The hypermethylated species however does not exhibit the expected Fe−C shortening. In contrast, these distances are elongated. This effect is particularly large for the weaker Fe−arene bond and is due to steric repulsions between the two substituted rings. In all cases the IP($^2E_2$) values are found to be lower than the IP($^2A_1$) values, their difference being lower in the case of the methylated species. Obviously, the presence of permethylation of the complex tends to preferencially destabilize the $e_2$ level. A nice linear correlation is found between the calculated IP's and the redox potentials within the $[Fe(C_5R_5)(C_6R'_6)]^+$ (R, R′ = H, Me) series (Figure 8). The increasing easiness of oxidation with the number of methyl groups is perfectly reproduced by the calculations. In addition, this correlation brings additional confidence in the reliability of the DFT results, and it allows the IP of any methylated complex to be evaluated from its redox potential and vice versa.

For example, the vertical IP values of [FeCp(mesitylene)]$^+$, **2**$^+$, and **4**$^+$ are expected be close to 12.7, 11.6, and 11.7 eV, respectively.

## Concluding Remarks

**1.** The family of 19-electron Fe$^I$ sandwich complexes related to **1** has been extensively used as an electron-reservoir system since both the 18-electron and 19-electron forms are stable.[3,27] Indeed these 19-electron complexes are the most electron-rich neutral molecules known on the basis of the values of their ionization potentials (**1**: 4.21 eV).[50] Their use has led to applications as stoichiometric single-electron-transfer reagents,[51a] initiators of electron-transfer-chain reactions,[51b] redox catalysts,[51c,52] medium-independent redox references,[52] and sensors.[53] This first report of the electrochemical oxidation of the 18-electron [FeCp(arene)]$^+$ cations and the first isolation of several 17-electron Fe$^{III}$ dications of this novel family opens the route to analogous stoichiometric and catalytic applications on the oxidation side.

**2.** The prototype 17-electron complex, [FeCp*($C_6Me_6$)]-[$SbX_6$]$_2$ (X = Cl or F), stable even in acetonitrile solution, has one of the highest redox potentials among oxidants which have ever been used (Table 2). In particular, it is the most oxidizing organometallic complex isolated so far. It has the advantage over $NO^+$ that it is a noncoordinating oxidant. Unlike Ce$^{IV}$ ammonium nitrate, it can be used in nonaqueous solvents. It compares to the $NAr_3^{\bullet+}$ salt family in that a large variety and number of substituents can be introduced on the rings to change the redox potential as shown in Table 1. Indeed the preliminary oxidation chemistry of [FeCp*($C_6Me_6$)][$SbCl_6$]$_2$ allowed us to generate and characterize spectroscopically for the first time new simple complexes such as [FeCp($\mu_3$-CO)]$_4$[$SbCl_6$]$_2$ (Scheme 2).

**3.** The three complexes **1**$^{2+}$, **1**$^+$, and **1** also form the first stable isostructural 17−18−19-electron triad of organometallic complexes. Moreover, the 17-electron complex [FeCp*($C_6Me_6$)][$SbX_6$]$_2$, (X = Cl or F) can be synthesized either from the 18-electron complex [FeCp*($C_6Me_6$)][$EX_6$] ($EX_6$ = $PF_6$, $SbCl_6$, or $SbF_6$) or from the 19-electron complex [FeCp*($C_6Me_6$)], the most reducing neutral complex known.[52] This provides direct interconversion between the three members of the 17−18−19-electron triad (Scheme 1).

**4.** The full characterization of [FeCp*($C_6Me_6$)][$SbX_6$]$_2$ and theoretical investigations allow the comparison of the $d^5$ electronic structure of the series of [FeCp(arene)]$^{2+}$ complexes with those of ferrocenium and [Fe($C_6H_6$)$_2$]$^{3+}$. The major difference is the additional charge that accounts for a redox potential 1.70 V more positive for the parent complex [FeCp-($C_6H_6$)]$^+$ than for ferrocene (Table 1). In fact, the dicationic [FeCp(arene)]$^{2+}$ complexes are the most oxidizing Fe$^{III}$ compounds known due to their high charge, and they can be viewed as superferrocenium derivatives. Although the 18-electron [FeCp(arene)]$^+$ species have their HOMO of $a_1$ symmetry, the ground state of their oxidized 17-electron parent is $^2E_2$, i.e. corresponding to the $(a_1)^2(e_2)^3$ configuration. The reason lies in the small energy difference between the $a_1$ and $e_2$ levels and in the significant Fe−arene bonding character of the $e_2$ level allowing geometric and electronic relaxation effects which stabilize this state.

**5.** In addition to providing a bonding analysis and detailed rationalization of the electrochemical and spectroscopic behavior of this series of complexes, the DFT calculations allowed the accurate determination of the molecular structures of [FeCp-($C_6H_6$)]$^{2+}$, [FeCp(anilin)]$^{2+}$, [$FeCp_2$]$^+$, and [Fe($C_6H_6$)$_2$]$^{3+}$ which are compared to that of their 18e parents.

**6.** The [Fe$^{II}$Cp(arene)]$^+$ complexes have an extremely rich functional chemistry that has led to the synthesis of a very large number of complexes.[20] This chemistry will now be extendable to the highly oxidizing Fe$^{III}$ oxidation state. An example with amino substituents on the arene ligand has been examined here, the Fe$^{II}$/Fe$^{III}$oxidation potential being significantly reduced with an important contribution of the iminocyclohexadienyl mesomer shown by DFT (Chart 1).

## Experimental Section

**General Data.** Reagent-grade tetrahydrofuran (THF), diethyl ether, and pentane were predried over Na foil and distilled from sodium-benzophenone ketyl under argon immediately prior to use. Acetonitrile ($CH_3CN$) was stirred under argon overnight over phosphorus pentoxide, distilled from sodium carbonate, and stored under argon. Methylene chloride ($CH_2Cl_2$) was distilled from calcium hydride just before use. All other chemicals were used as received. All manipulations were carried out with Schlenk techniques or in a nitrogen-filled Vacuum Atmospheres drylab. Infrared spectra were recorded with a Perkin-Elmer 1420 ratio recording infrared spectrophotometer that was calibrated with polystyrene. Samples were examined in solution (0.1 mm cells with NaCl windows), between NaCl disks in Nujol, or in KBr pellets. $^1$H NMR spectra were recorded with a Brucker AC 200 (200 MHz) spectrometer. $^{13}$C NMR spectra were obtained in the pulsed FT mode at 50.327 MHz with a Brucker AC 200 spectrometer. All chemical shifts are reported in parts per million ($\delta$, ppm) with reference to the solvent or $Me_4Si$. Electronic spectra (UV and visible) were recorded at 20 °C with a Cary 219 spectrophotometer with 10 or 1 mm quartz cells. Cyclic voltammetry data were recorded with a PAR 273 potentiostat galvanostat. Care was taken in the CV experiments to minimize the effects of solution resistance on the measurements of peak potentials (the use of positive feedback *iR* compensation and dilute solution ($\approx 10^{-3}$ mol/L) maintained currents between 1 and 10 $\mu$A).[25,2] The additional redox couple [$FeCp_2$]/[$FeCp_2$]$^+$ was used when possible as a control for *iR* compensation. Thermodynamic potentials were recorded with reference to an aqueous SCE in THF (0.1 M *n*-$Bu_4NBF_4$). When necessary, the reference electrode was an Ag *quasi*-reference electrode (QRE). The silver wire was pretreated by immersion in 10 M $HNO_3$ for 5 min before use. The value of the [$FeCp_2$]/[$FeCp_2$]$^+$ redox couple was 0.08 V vs Ag in $SO_2$, 0.382 V *vs* SCE on Pt in MeCN, and 0.475 V vs SCE on Pt in $CH_2Cl_2$. The QRE potential was calibrated by adding the reference couple [$FeCp_2$]/[$FeCp_2$]$^+$. The counter electrode was platinum. Mössbauer spectra were recorded with a 25 mCi $^{57}$Co source on Rh, using a symmetric triangular sweep mode. Elemental analyses were performed by the Centre of Microanalyses of the CNRS at Lyon-Villeurbanne, France.

**Preparation of 1[$SbCl_6$]$_2$. (1) From 1**: A sample of **1**[$PF_6$] (0.498 g, 1 mmol) in 10 mL of THF was stirred with 10 g of sodium amalgam (0.8%). The reduction was achieved in 1 h. THF was then removed in vacuo and the residue was extracted with pentane (2 × 15 mL). Pentane was then removed in vacuo which left a dark green product **1** (0.307 g, 87% yield). The complex **1** (neat) was cooled to −80 °C and 5 mmol of $SbCl_5$ (1 M solution in $CH_2Cl_2$) at −80 °C were added under magnetic stirring. The reaction mixture was then slowly warmed to room temperature and a brown solution and a purple precipitate appeared. The solution was then transferred by cannula, and the solid residue was washed with $CH_2Cl_2$ (4 × 15 mL) and recrystallized from $SO_2$ at −40 °C, which yielded the complex **1**[$SbCl_6$]$_2$ as a microcrystalline purple powder (0.694 g, 78% yield). Analysis for **1**[$SbCl_6$]$_2$. Calcd for $C_{22}H_{33}FeSb_2Cl_{12}$: C, 25.85; H, 3.25. Found: C, 25.84; H,

(50) Green, J. C.; Kelly, M. R.; Payne, M. P.; Seddon, E. A.; Astruc, D.; Hamon, J.-R.; Michaud, P. *Organometallics* **1983**, *2*, 211−218.
(51) (a) Reference 3, Chapter 5. (b) Reference 3, Chapter 6. (c) Reference 3, Chapter 7.
(52) Juiz, J.; Astruc, D. *C. R. Acad. Sci. Ser. II* **1998**, 21.
(53) Valério, C.; Fillaut, J.-L.; Ruiz, J.; Guittard, J.; Blais, J.-C.; Astruc, D. *J. Am. Chem. Soc.* **1997**, *119*, 2588.

3.47. UV−vis for **1**[$SbCl_6$]$_2$: $\lambda_{max}$ (MeCN) 487 nm ($\epsilon$ = 228 L·M$^{-1}$·cm$^{-1}$); $\lambda_{max}$ (MeCN) 525 nm ($\epsilon$ = 213 L·M$^{-1}$·cm$^{-1}$).

**(2) From 1[$PF_6$]:** To **1**[$PF_6$] (0.498 g, 1 mmol) in 10 mL of $CH_2Cl_2$ under argon was added 5 mmol of $SbCl_5$ (1 M solution in $CH_2Cl_2$) with magnetic stirring. Formation of a purple precipitate from the initially yellow solution was instantaneous. The purple solid was filtered and washed with $CH_2Cl_2$ (4 × 15 mL) until the latter was colorless, then recrystallized from $SO_2$ at −40 °C (0.624 g, 71% yield, Anal. C, H).

**Preparation of 2[$SbCl_6$]$_2$.** **2**[$SbCl_6$]$_2$ was prepared as above, starting from **2**[$PF_6$]. The reaction time for complete color change was 1 min. After washing 4 times with 20 mL of $CH_2Cl_2$ and recrystallizing from $SO_2$, **2**[$SbCl_6$] was obtained in 70% yield. Anal. Calcd for $C_{21}H_{31}FeSb_2F_{12}$: C, 25.02; H, 3.10. Found: C, 25.15; H, 3.42.

**Generation of 4[$SbCl_6$]$_2$.** Application to **4**[$PF_6$] of the above procedure led to a color change from yellow to brown in 0.5 h. Washing with 10 × 20 mL of $CH_2Cl_2$ did not give colorless $CH_2Cl_2$ solution; an EPR spectrum of the remaining orange-purple solid (10%) was recorded. This spectrum was identical to those of **1**[$SbCl_6$]$_2$ and **2**[$SbCl_6$]$_2$ (see text).

**Preparation of 1[$SbF_6$]$_2$. (1) Using $SbF_5$.** A cold solution (−40 °C) of **1**[$SbF_6$] (0.295 g, 0.5 mmol) in $SO_2$ (10 mL) was added to a cold solution (−40 °C) of $SbF_5$ (1 mmol) in $SO_2$ (10 mL) and the color immediately changed from yellow to purple. The solvent was evaporated while the solution was then allowed to warm. Then, the brown-purple solid residue was washed several times with $CH_2Cl_2$ until $CH_2Cl_2$ was colorless, which gave 72% (0.297 g) of **1**[$SbF_6$]$_2$ as a purple powder. Analysis for **1**[$SbF_6$]$_2$. Calcd for $C_{22}H_{33}FeSb_2F_{12}$: C, 32.04; H, 4.03. Found: C, 32.35; H, 4.50.

**(2) Using $Br_2$ and [Ag][$SbF_6$].** The complex **1**[$SbF_6$] (0.295 g, 0.5 mmol) was stirred in 10 mL of $CH_2Cl_2$ with [Ag][$SbF_6$] (0.344 g, 1 mmol) at 20 °C. Then $Br_2$ (solution: 1 mmol in 5 mL of $CH_2Cl_2$) was added, and a purple precipitate immediately formed. The solvent was then evaporated in vacuo and the residue was extracted with $CH_3CN$ (10 mL). The reaction mixture was filtrered and the solvent was removed in vacuo. The residue was washed with $CH_2Cl_2$ (2 × 5 mL), giving a dark purple powder of **1**[$SbF_6$]$_2$ (0.186 g, 45% yield, Anal. C, H).

**Single-Electron Oxidation of [FeCp($\mu_3$-CO)]$_4$ with 1[$SbCl_6$]$_2$.** [FeCp($\mu_3$-CO)]$_4$ (59.6 mg, 0.1 mmol) in 10 mL of $CH_2Cl_2$ was stirred with **1**[$SbCl_6$]$_2$ (128 mg, 0.125 mmol). The color of the solution turned from green to orange. After 2 h, the solution was cooled to −40 °C and filtered. The precipitate was washed with 4 × 5 mL of cold $CH_2Cl_2$. The black green powder [FeCp($\mu_3$-CO)]$_4$[$SbCl_6$] was obtained in 86% yield (80 mg, 0.086 mmol) and characterized by infrared ($\nu_{CO}$ = 1674 cm$^{-1}$) and reduction back to the neutral cluster with [FeCp*$_2$]. The orange $CH_2Cl_2$ solution was passed through a short alumina column and **1**[$SbCl_6$] was eluted with $CH_2Cl_2$, which gave 76.5 mg (0.111 mmol, 89% yield) of product.

**Two-Electron Oxidation of [FeCp($\mu_3$-CO)]$_4$ with 1 [$SbCl_6$]$_2$.** A dark-purple powder of **1**[$SbCl_6$]$_2$ (611 mg, 0.5 mmol) was added to a solution of [FeCp($\mu_3$-CO)]$_4$ (119 mg, 0.2 mmol) in 30 mL of $CH_2Cl_2$. After the solution was stirred overnight at room temperature, a brown orange solution and a black precipitate appeared. The solution was transferred to a Schlenk flask and the remaining black powder was washed with 4 × 5 mL of $CH_2Cl_2$ until $CH_2Cl_2$ was colorless, which gave 215 mg (0.17 mmol, 85% yield) of [FeCp($\mu_3$-CO)]$_4$[$SbCl_6$]$_2$ ($\nu_{CO}$ = 1733 cm$^{-1}$, vs; $\nu_{CO}$ = 1787 cm$^{-1}$, s). Upon exposure of the black dication to air, [FeCp($\mu_3$-CO)]$_4$[$SbCl_6$] slowly formed ($\nu_{CO}$ = 1674 cm$^{-1}$). The integrity of the mono- and dicationic clusters was checked by reduction back to the neutral cluster (vide infra). The filtrate was passed through a short alumina column and **1**[$SbCl_6$] was eluted with $CH_2Cl_2$, which gave 316 mg (0.46 mmol, 92% yield). [FeCp($\mu_3$-CO)]$_4$[$SbCl_6$]$_2$ was slightly thermally unstable and decomposed over several days giving inter alia a monometallic [FeCp(CO)$_3$]$^+$ salt characterized by the known strong infrared bands at 2071 and 2120 cm$^{-1}$.[36c−e]

**Reduction of [FeCp($\mu_3$-CO)]$_4$[$SbCl_6$]$_2$.** [FeCp*$_2$] (0.2 mmol, 65 mg) was added to a stirred suspension of [FeCp($\mu_3$-CO)]$_4$[$SbCl_6$]$_2$ (114 mg, 0.09 mmol) in $CH_2Cl_2$ (10 mL). After 5 min, the color of the solution became green and homogeneous. The solution was passed through a short alumina column giving two green bands. The first one was that of the neutral cluster [FeCp($\mu_3$-CO)]$_4$ ($\nu_{CO}$ = 1623 cm$^{-1}$), which was eluted with $CH_2Cl_2$ (0.064 mmol, 38 mg, 71%). The second one was that of [FeCp*$_2$][$SbCl_6$], which was eluted with 10% MeOH in $CH_2Cl_2$ (v/v) (126 mg, 0.19 mmol, 95% yield). This complex was characterized by its single-electron reduction to [FeCp*$_2$] with [FeCp($C_6Me_6$)].

**Single-Electron Oxidation of [Ru(bpy)$_3$][$PF_6$]$_2$ and Generation of [Ru(bpy)$_3$]$^{3+}$ with 1[$SbCl_6$]$_2$.** A dark-purple powder of **1**[$SbCl_6$]$_2$ and the orange $CH_2Cl_2$ solution of [Ru(bpy)$_3$][$PF_6$]$_2$ (stoichiometric amounts, 10$^{-3}$ M) were introduced in an EPR tube under argon. A green precipitate appeared after a few minutes at room temperature; its EPR spectrum was recorded at 4 K and showed the three signals of [Ru(bpy)$_3$]$^{3+}$: $g$ = 2.649, 2.068, 1.377.[34]

**Redox Catalysis of the Anodic Oxidation of Furfural by [FeCp($C_6Me_6$)][$PF_6$].** In the conventional electrochemical cell for voltammetric studies, 20 mL of $SO_2$, [$n$-$Bu_4N$][$PF_6$] 0.1 M, and 5.9 mg (0.0137 mmol) of [FeCp($C_6Me_6$)][$PF_6$] were added at −40 °C. Three voltammograms were recorded at scan rates of 0.1, 0.2, and 0.3 V·s$^{-1}$. Furfural (116 mg, 1.207 mmol) was added and three new voltammograms were recorded at the same scan rates, showing an enhancement of the oxidation wave of [FeCp($C_6Me_6$)][$PF_6$]. The rate constant calculated from the intensity enhancement of this oxidation wave with the Nicholson-Shain equation[37b] under these conditions was $k$ = 115 mol·L$^{-1}$·s$^{-1}$.

**Computational Details.** The DFT calculations were carried out by using the ADF program developped by Baerends et al.[58] The geometries of the 18-electron methylated complexes [Fe($C_5R_5$)($C_6R'_6$)]$^+$ (R, R′ = H, Me) were optimized within the local density approximation (LDA) of the Kohn−Sham equations[59] by using the Slater exchange[60] and Vosko−Wilk−Nusair[61] correlation potentials. These optimized geometries were used for the calculations of the ionization potentials by using the transition state method[49] at the nonlocal density approximation (NLDA) for which the Becke exchange[62] and Perdew correlation[63] corrections were added to the local potentials. All the calculations on the [$FeCp_2$]$^{0/+}$, [Fe($C_6H_6$)$_2$]$^{2+/3+}$, [FeCp($C_6H_6$)]$^{+/2+}$, and [FeCp($C_6H_5NH_2$)]$^{+/2+}$ complexes were carried out within the same NLDA approximation. All the 17-electron species were calculated under the spin-polarized formalism.

The ADF atomic basis sets III and IV were used for the light elements and for iron, respectively.[64] They correspond to the uncontracted double-$\zeta$ Slater-type orbital (STO) basis set for the valence orbitals of C and H, augmented by one 2p function for H and by one 3p function for C.[64] In the case of Fe, an uncontracted triple-$\zeta$ STO basis set was used for the 4s and 3d orbitals. The 4p orbitals were described by simple-$\zeta$ STOs. The cores (C: 1s; Fe: 1s−3p) were treated by the frozen-core approximation.[58a] A set of auxiliary s, p, d, f, and g functions centered on all nuclei was used to fit the molecular density.

The geometries of the 18-electron complexes [$FeCp_2$] and [Fe($C_6H_6$)$_2$]$^{2+}$ were optimized under the $C_{5v}$ and $C_{6v}$ symmetry constraints, respectively. In the case of ferrocene, the eclipsed conformation was found to be more stable than the staggered one by 0.036 eV. In the case of [Fe($C_6H_6$)$_2$]$^{2+}$, the staggered conformation is calculated to be preferred by only 0.005 eV. An even lower rotational barrier was computed for [FeCp($C_6H_6$)]$^+$ (0.002 eV), for which the energy minimum

(54) Droege, M. W.; Harman, W. D.; Taube, H. *Inorg. Chem.* **1987**, *26*, 1309.
(55) Lochynski, S.; Shine, H. J.; Siroka, M.; Venkatachalam, T. K. *J. Org. Chem.* **1990**, *55*, 2702.
(56) Baker, P. K.; Connelly, N. G.; Jones, B. M. R.; Maher, J. P.; Somers, K. R. *J. Chem. Soc., Dalton Trans.* **1980**, 579.
(57) Bohling, D. A.; Mann, K. R. *Inorg. Chem.* **1983**, *22*, 1561.
(58) (a) Baerends, D. E.; Hellis, D. E.; Ros, P. *Chem. Phys.* **1973**, *2*, 41. (b) Baerends, E. J.; Ros, P. *Int. Quantum Chem.* **1978**, *S12*, 169. (c) te Velde, G.; Baerends, D. E. *J. Comput. Phys.* **1992**, *99*, 84.
(59) Kohn, W.; Sham, L. *J. Phys. Rev.* **1965**, *A140*, 1133.
(60) Slater, J. C. *Quantum Theory of Molecules and Solids*; MacGraw-Hill: New York, 1974; Vol. 4.
(61) Vosko, S. H.; Wilk, L.; Nusair, M. *Can. J. Phys.* **1965**, *58*, 1200.
(62) Becke, A. D. *Phys. Rev.* **1988**, *A38*, 3098.
(63) Perdew, J. P. *Phys. Rev.* **1986**, *B33*, 8822.
(64) Snjiders, G.; Baerends, E. J.; Vernoojs, P. *At. Nucl. Data Tables* **1982**, *26*, 483.

corresponds to a conformation of $C_s$ symmetry in which each of the two rings are eclipsed at one of their carbon atoms (see $C_s(1)$ in Chart 3). These energy barriers are not significantly different from zero at the considered level of theory. Owing to this almost free rotation of the rings in the 18-electron complexes, the rotational conformation was not optimized in the case of the 17-electron species $[FeCp_2]^+$ and $[Fe(C_6H_6)_2]^{3+}$, but was fixed as being the same as that found for their 18-electron parents, i.e. eclipsed and staggered, respectively. In the case of $[FeCp(C_6H_6)]^{2+}$, the two possible $C_s$ conformations were considered (see Chart 3). The $^2E_2$ states of $[FeCp_2]^+$ and $[Fe(C_6H_6)_2]^{3+}$ were computed assuming the $C_{2v}$ and $D_2$ symmetry, respectively. This renders symmetry-equivalent the two rings, through a mirror and a $C_2$ axis in the case of $[FeCp_2]^+$ and though two $C_2$ axes in the case of $[Fe(C_6H_6)_2]^{3+}$. The $C_{5v}$, $C_{6v}$, and $C_s$ symmetries were imposed for $^2A_1$ states of $[FeCp_2]^+$, $[Fe(C_6H_6)_2]^{3+}$, and $[FeCp(C_6H_6)]^{2+}$, respectively. In the two former cases, as for the 18-electron parents, no significant distortion away from the ideal $D_{5h}$ and $D_{6d}$ symmetries was found. In the latter case, convergence problems occurred which could be overcome only for the $C_s(1)$ conformation. The calculations of the $[FeCp(C_6H_5NH_2)]^{+/2+}$ complexes were carried out assuming the $C_s(1)$ conformation, as well as the NLDA optimization of the 18-electron series $[Fe(C_5R_5)(C_6R'_6)]^+$ (R, R′ = H, Me).

**Acknowledgment.** Dedicated to Prof. Peter Jutzi on the occasion of his 60th birthday. Helpful discussion with Professor P. R. Sharp concerning the use of $SO_2$, assistance for ESR spectroscopy by Professor C. Coulon, a gift of **3**$[PF_6]_2$ by Dr. M.-H. Delville, computing facilities by the Centre de Ressources Informatiques (CRI) of Rennes and the Institut de Développement et de Ressources en Informatique Scientifique (IDRIS-CNRS) of Orsay, and research support by the Institut Universitaire de France (D.A.), the Centre National de la Recherche Scientifique, and the Universities of Bordeaux I, Rennes 1 and Versailles are gratefully acknowledged.

JA982342Z